

RESEARCH ARTICLE

Rho-associated kinase and zipper-interacting protein kinase, but not myosin light chain kinase, are involved in the regulation of myosin phosphorylation in serum-stimulated human arterial smooth muscle cells

Jing-Ti Deng, Sabreena Bhaidani, Cindy Sutherland, Justin A. MacDonald, Michael P. Walsh¹*

Department of Biochemistry & Molecular Biology, Cumming School of Medicine, University of Calgary, Calgary, Alberta, Canada

* walsh@ucalgary.ca



OPEN ACCESS

Citation: Deng J-T, Bhaidani S, Sutherland C, MacDonald JA, Walsh MP (2019) Rho-associated kinase and zipper-interacting protein kinase, but not myosin light chain kinase, are involved in the regulation of myosin phosphorylation in serum-stimulated human arterial smooth muscle cells. *PLoS ONE* 14(12): e0226406. <https://doi.org/10.1371/journal.pone.0226406>

Editor: Salvatore V Pizzo, Duke University School of Medicine, UNITED STATES

Received: May 27, 2019

Accepted: November 26, 2019

Published: December 13, 2019

Copyright: © 2019 Deng et al. This is an open access article distributed under the terms of the [Creative Commons Attribution License](https://creativecommons.org/licenses/by/4.0/), which permits unrestricted use, distribution, and reproduction in any medium, provided the original author and source are credited.

Data Availability Statement: All relevant data are within the paper and its Supporting Information files.

Funding: This work was supported by grants MOP-111262 to MPW and MOP-133494 to JAM from The Canadian Institutes of Health Research (<http://www.cihr-irsc.gc.ca>). The funders had no role in study design, data collection and analysis, decision to publish, or preparation of the manuscript.

Abstract

Myosin regulatory light chain (LC₂₀) phosphorylation plays an important role in vascular smooth muscle contraction and cell migration. Ca²⁺/calmodulin-dependent myosin light chain kinase (MLCK) phosphorylates LC₂₀ (its only known substrate) exclusively at S19. Rho-associated kinase (ROCK) and zipper-interacting protein kinase (ZIPK) have been implicated in the regulation of LC₂₀ phosphorylation via direct phosphorylation of LC₂₀ at T18 and S19 and indirectly via phosphorylation of MYPT1 (the myosin targeting subunit of myosin light chain phosphatase, MLCP) and Par-4 (prostate-apoptosis response-4). Phosphorylation of MYPT1 at T696 and T853 inhibits MLCP activity whereas phosphorylation of Par-4 at T163 disrupts its interaction with MYPT1, exposing the sites of phosphorylation in MYPT1 and leading to MLCP inhibition. To evaluate the roles of MLCK, ROCK and ZIPK in these phosphorylation events, we investigated the time courses of phosphorylation of LC₂₀, MYPT1 and Par-4 in serum-stimulated human vascular smooth muscle cells (from coronary and umbilical arteries), and examined the effects of siRNA-mediated MLCK, ROCK and ZIPK knockdown and pharmacological inhibition on these phosphorylation events. Serum stimulation induced rapid phosphorylation of LC₂₀ at T18 and S19, MYPT1 at T696 and T853, and Par-4 at T163, peaking within 30–120 s. MLCK knockdown or inhibition, or Ca²⁺ chelation with EGTA, had no effect on serum-induced LC₂₀ phosphorylation. ROCK knockdown decreased the levels of phosphorylation of LC₂₀ at T18 and S19, of MYPT1 at T696 and T853, and of Par-4 at T163, whereas ZIPK knockdown decreased LC₂₀ diphosphorylation, but *increased* phosphorylation of MYPT1 at T696 and T853 and of Par-4 at T163. ROCK inhibition with GSK429286A reduced serum-induced phosphorylation of LC₂₀ at T18 and S19, MYPT1 at T853 and Par-4 at T163, while ZIPK inhibition by HS38 reduced only LC₂₀ diphosphorylation. We also demonstrated that serum stimulation induced phosphorylation (activation) of ZIPK, which was inhibited by ROCK and ZIPK down-regulation and inhibition. Finally, basal phosphorylation of LC₂₀ in the absence of serum stimulation was

Competing interests: The authors have declared that no competing interests exist.

unaffected by MLCK, ROCK or ZIPK knockdown or inhibition. We conclude that: (i) serum stimulation of cultured human arterial smooth muscle cells results in rapid phosphorylation of LC₂₀, MYPT1, Par-4 and ZIPK, in contrast to the slower phosphorylation of kinases and other proteins involved in other signaling pathways (Akt, ERK1/2, p38 MAPK and HSP27), (ii) ROCK and ZIPK, but not MLCK, are involved in serum-induced phosphorylation of LC₂₀, (iii) ROCK, but not ZIPK, directly phosphorylates MYPT1 at T853 and Par-4 at T163 in response to serum stimulation, (iv) ZIPK phosphorylation is enhanced by serum stimulation and involves phosphorylation by ROCK and autophosphorylation, and (v) basal phosphorylation of LC₂₀ under serum-free conditions is not attributable to MLCK, ROCK or ZIPK.

Introduction

Phosphorylation at S19 of the 20-kDa regulatory light chains of myosin II (LC₂₀), catalyzed by myosin light chain kinase (MLCK), is the trigger for smooth muscle contraction [1–4]. Smooth muscle MLCK is capable of phosphorylating T18 of LC₂₀ in addition to S19 [5,6]; however, this has only been demonstrated *in vitro* at high kinase concentrations (a high MLCK: myosin II ratio), and abundant evidence indicates that it does not occur *in situ* [7,8]. In some instances, however, LC₂₀ is phosphorylated at both T18 and S19 in vascular smooth muscle tissue. For example, in renal afferent arterioles of the rat, the pathophysiological stimulus endothelin-1 induces diphosphorylation of LC₂₀ at T18 and S19, whereas the physiological stimulus angiotensin II induces exclusively monophosphorylation at S19 [9]. Diphosphorylation is associated with a decrease in the rate of dephosphorylation of LC₂₀ by myosin light chain phosphatase (MLCP) and, therefore, prolongation of the contractile response [10]. LC₂₀ diphosphorylation has also been observed frequently in cultured smooth muscle and endothelial cells [11–13]. The observation that LC₂₀ diphosphorylation occurs in response to treatment with membrane-permeant phosphatase inhibitors indicates that blocking phosphatase activity unmasks basal activity of endogenous kinase(s) that phosphorylate LC₂₀ at T18 and S19 [14]. These findings raise the question: which kinase(s) is responsible for phosphorylation of LC₂₀ at T18 and S19? Candidate kinases include Rho-associated coiled-coil kinase (ROCK) [15], zipper-interacting protein kinase (ZIPK) [16–20], integrin-linked kinase (ILK) [21,22] and citron kinase (a Rho-dependent kinase related to ROCK) [23]. In this study, we followed the time courses of phosphorylation of LC₂₀ and of proteins implicated in the regulation of myosin light chain phosphorylation, the myosin targeting subunit of MLCP (MYPT1), prostate-apoptosis response-4 (Par-4) and ZIPK itself, in serum-stimulated human cultured vascular smooth muscle cells from coronary artery and umbilical artery. We then investigated the effects of MLCK, ROCK and ZIPK knockdown and pharmacological inhibition on the serum-induced phosphorylation of LC₂₀, MYPT1, Par-4 and ZIPK.

Materials and methods

Materials

All chemicals were reagent grade unless indicated otherwise. H1152 ((S)-(+)-2-methyl-1-[(4-methyl-5-isoquinoliny) sulfonyl]-hexahydro-1H-1,4-diazepine dihydrochloride), a selective ROCK inhibitor [24] purchased from Calbiochem (catalog number 555550), was used at 200 nM; it also inhibits, but with lower potency, PRK2 and other members of the AGC subfamily of protein kinases such as RSK1, RSK2, PKA, MSK1 [25] and LRRK2 [26].

GSK429286A (*N*-(6-fluoro-1H-indazol-5-yl)-2-methyl-6-oxo-4-(4-(trifluoromethyl)phenyl)-1,4,5,6-tetrahydropyridine-3-carboxamide), a more selective ROCK inhibitor that does not inhibit LRRK2, was used at 1 μ M [26] and was purchased from Selleckchem (Houston, TX; cat. no. S1474). HS38 (2-((1-(3-chlorophenyl)-4-oxo-4,5-dihydro-1H-pyrazolo[3,4-*d*]-pyrimidin-6-yl)thio)propanamide), a ZIPK inhibitor [27,28], was generously provided by Dr. Tim Haystead (Duke University). HS38 has no effect on ROCK activity [29], unlike other commercially available compounds such as TC-DAPK6 [29,30]; HS38 does, however, inhibit PIM kinases and IRAK4 [27]. Wortmannin, purchased from Calbiochem (cat. no. W1628), was used at a concentration of 1 μ M, at which it is a highly selective inhibitor of PI 3-kinase and MLCK [31]. ML7 (1-(5-iodonaphthalene-1-sulfonyl)-1H-hexahydro-1,4-diazepine hydrochloride), a selective MLCK inhibitor purchased from Calbiochem (cat. no. I2764), was used at 20 μ M [32].

Human arterial smooth muscle cell cultures

Human coronary artery smooth muscle cells (CASMC: CC-2583) and human umbilical artery smooth muscle cells (UASMC: CC-2579), purchased from Lonza (Basel, Switzerland), were cultured in smooth muscle growth medium (Lonza SmGM-2: CC-3182) containing 5% fetal bovine serum (FBS), growth factors (hEGF, insulin and hFGF- β), gentamicin and amphotericin-B at 37 °C in a humidified incubator with 5% CO₂. These cells maintain their morphological and phenotypic characteristics for up to 10 passages and were, therefore, used for experiments within 10 passages. Cells were plated at a density of 2 X 10⁵ cells/ml into 4-well plates (Nunc, Thermo Scientific, Waltham, MA) with smooth muscle growth medium containing 5% FBS. Prior to treatment, cells were grown to 70% confluence and starved in FBS-free medium overnight. Cells were then stimulated with 5% FBS for times indicated in the figures (typically 0, 15 s, 30 s, 1 min, 2 min, 5 min, 30 min, 1 h and 2 h) to observe their various responses to FBS. The treated cells were lysed immediately in Laemmli sample buffer and heated at 90 °C for 5 min. To investigate the effects of kinase inhibitors, cells were starved in FBS-free medium for 8 h to induce cell quiescence and then incubated with various inhibitors for \geq 45 min prior to stimulation with 5% FBS for 2 min and then lysed in Laemmli sample buffer.

siRNA-mediated knockdown

CASMC and UASMC were transfected with human ROCK1, ZIPK or MLCK siRNAs or negative control siRNA (see below) using HiPerFect Reagent (Qiagen, Hilden, Germany) according to the manufacturer's protocol, as previously described in detail [33]. Human ROCK1 siRNA, purchased from Santa Cruz Biotechnology (Santa Cruz, CA; cat. no. sc-29473), consists of three target-specific siRNAs (19–25 nucleotides). Human ZIPK siRNA, purchased from Ambion/Thermo Fisher Scientific (Waltham, MA; part number 4390824, siRNA ID #s559, Lot #ASO0UMMU), has the following sequence:

sense: 5' -GAGGAGUACUUCAGCAACAAtt-3'

antisense: 5' -UGUUGCUGAAGUACUCCUCgt-3'.

Human MLCK siRNA, purchased from Ambion/Thermo Fisher Scientific (part number 4392420, siRNA ID#s9193, Lot #ASO0T348), has the following sequence:

sense: 5' -GCCUCAUGUAAAACCCUAUttt-3'

anti-sense: 5' -AUAGGGUUUUACAUGAGGCttt-3'.

Negative control siRNA (Ambion negative control #2, part #AM4613) contains sequences that do not target any gene product.

Western blotting

Cells were lysed in Laemmli sample buffer (65 mM Tris-HCl, pH 6.8, 10% glycerol, 3% SDS, 1% β -mercaptoethanol, 0.04% bromophenol blue) following treatments indicated in the Results section, heated at 90 °C for 5 min and resolved by SDS-PAGE (11% acrylamide). Proteins were transferred to nitrocellulose membranes in 25 mM Tris, 192 mM glycine, 20% methanol overnight at 30 V and 4 °C. Membranes were blocked with 5% non-fat dry milk in 25 mM Tris-HCl, pH 7.4, 150 mM NaCl, 0.05% Tween-20 (TBST) for 1 h at 20 °C. Membranes were incubated for 2 h at 20 °C with primary antibody in 1% milk in TBST, washed, incubated with horseradish peroxidase (HRP)-conjugated goat polyclonal anti-rabbit IgG (1:100,000 dilution; EMD Millipore (Etobicoke, Ontario, Canada); cat. no. AP132P) or donkey anti-goat IgG-HRP (1:100,000 dilution; Santa Cruz Biotechnology; cat. no. sc-2020) in 1% milk in TBST and washed 3 times with TBST. Blots were developed with Supersignal West Femto enhanced chemiluminescence substrate (Thermo Scientific). Emitted light was detected and quantified with a chemiluminescence imaging analyzer (LAS3000mini; Fujifilm, Tokyo, Japan) and images were analyzed with MultiGauge version 3.0 software (Fujifilm). Protein levels were expressed relative to a standard (GAPDH, SM22 α or α -actin) as indicated in the text. The following primary antibodies were used in this study: rabbit monoclonal anti-ZIPK (1:1,000 dilution; Epitomics, Burlingame, CA; cat. no. 2568-1), rabbit polyclonal anti-ROCK1 (1:1,000 dilution; Epitomics; cat. no. S2711), rabbit polyclonal anti-ROCK2 (1:2,000 dilution; AbFrontier, Seoul, South Korea; cat. no. LF-PA0049), rabbit polyclonal anti-pT18/pS19-myosin light chain 2 (1:500 dilution; Cell Signaling; cat. no. 3674), rabbit anti-GAPDH (1:5,000 dilution; Santa Cruz Biotechnology; cat. no. sc-32233), goat polyclonal anti-SM22 α (1:2,500 dilution; Novus Biologicals, Centennial, CO; cat. no. NB600-507), rabbit polyclonal anti-LC₂₀ (1:2,000 dilution; Rockland Immunochemicals, Limerick, PA; cat. no. 600-401-938), rabbit polyclonal anti-pT853-MYPT1 (1:1,000 dilution; EMD Millipore; cat. no. 36-003), rabbit polyclonal anti-pT696-MYPT1 (1:1,000 dilution; EMD Millipore; cat. no. ABS45), rabbit polyclonal anti-pT163-Par4 (1:1,000 dilution; Cell Signaling; cat. no. 2329), rabbit monoclonal anti-pS473-Akt (193H12) (1:1,000 dilution; Cell Signaling; cat. no. 4058); rabbit polyclonal anti-pT180/pY182-p38 MAP kinase (1:1,000 dilution; Cell Signaling; cat. no. 9211), rabbit monoclonal anti-pT202/Y204-ERK1/pT185/pY187-ERK2 (1:1,000 dilution; Cell Signaling; cat. no. 4370), rabbit anti-pS82-HSP27 (1:1,000 dilution; Cell Signaling; cat. no. 2401), and rabbit polyclonal anti- α -actin (1:1,000 dilution; Cytoskeleton, Inc.; cat. no. AAN01). Polyclonal antibodies to purified, full-length chicken gizzard MLCK were raised in rabbits [34].

Phosphate affinity SDS-PAGE (Phos-tag SDS-PAGE)

The phosphorylation of LC₂₀ and ZIPK was analyzed by phosphate-binding tag SDS-PAGE [35]. For LC₂₀ phosphorylation analysis, samples were resolved in SDS gels containing 12% acrylamide, 40 μ M Phos-tag reagent and 0.1 mM MnCl₂ at 20 mA/gel. Separated proteins were transferred to PVDF membranes (Roche Applied Science, Penzberg, Germany) overnight at 28 V and 4 °C in 25 mM Tris-HCl, pH 7.5, 192 mM glycine, 10% (v/v) methanol. Proteins were fixed on the membrane by treatment with 0.5% glutaraldehyde in phosphate-buffered saline (137 mM NaCl, 2.68 mM KCl, 10 mM Na₂HPO₄, 1.76 mM KH₂PO₄) for 30 min. For ZIPK phosphorylation analysis, samples were separated in SDS gels containing 6.5% acrylamide, 55 μ M Phos-tag reagent and 0.1 mM MnCl₂ (or 1–2 mM EDTA) at 20 mA/gel. Separated proteins were transferred to nitrocellulose membranes in 25 mM Tris-HCl, pH 7.5, 192 mM

glycine, 20% (v/v) methanol at 28 V for 18 h at 4 °C. Membranes were then blocked with 5% non-fat dry milk in TBST for 1 h at 20 °C, washed with water and TBST and incubated for 2 h with primary antibody (anti-ZIPK in Can Get Signal (Immunoreaction Enhancer Solution 1; Toyobo Life Science Department, Osaka, Japan) prior to further washing in water and TBST and incubation for 1 h with secondary antibody in 1% (w/v) non-fat dry milk in TBST. Immunoreactive bands were detected with SuperSignal West Femto Maximum Sensitivity Substrate (Thermo Fisher Scientific).

Data analysis

Values are presented as mean \pm SEM, with n indicating the number of independent experiments performed. Statistically significant differences were determined by Student's unpaired t -test or Dunnett's *post hoc* test for multiple comparisons as indicated in the text and figure legends. Statistically significant differences were indicated by $p < 0.05$.

Results

Serum-induced phosphorylation of LC₂₀

Analysis of LC₂₀ phosphorylation in serum-starved human coronary and umbilical arterial smooth muscle cells by Phos-tag SDS-PAGE, which separates unphosphorylated, mono- and diphosphorylated LC₂₀ species [10], revealed a significant basal level of phosphorylation: 0.55 ± 0.05 mol P_i/mol LC₂₀ ($n = 7$) in CASMC and 0.85 ± 0.02 mol P_i/mol LC₂₀ ($n = 6$) in UASMC (time zero samples in Fig 1B and 1D, respectively). Most of the basal phosphorylation under these conditions was at a single site, although diphosphorylated LC₂₀ was also detected (time zero samples in Fig 1A and 1C). Serum stimulation induced a rapid increase in phosphorylation to a peak of 1.12 ± 0.08 mol P_i/mol LC₂₀ ($n = 7$) in CASMC (Fig 1A and 1B) and 1.33 ± 0.02 mol P_i/mol LC₂₀ ($n = 6$) in UASMC (Fig 1C and 1D) at 2 min after serum addition. In the case of CASMC, this level of LC₂₀ phosphorylation was sustained for a prolonged period of time; the value after 2 h serum stimulation was 0.97 ± 0.03 mol P_i/mol LC₂₀ ($n = 7$), not significantly different from the value at 2 min ($p = 0.09$; Student's unpaired t -test) (Fig 1B), whereas it declined significantly over this period in UASMC to 1.02 ± 0.04 mol P_i/mol LC₂₀ ($n = 6$), significantly lower than the value at 2 min ($p < 0.001$; Student's unpaired t -test) (Fig 1D). Analysis of LC₂₀ diphosphorylation using phosphospecific antibodies that recognize LC₂₀ only when phosphorylated at both T18 and S19 confirmed a low level of basal diphosphorylation under serum-free conditions, which increased rapidly in both CASMC (Fig 2A) and UASMC (Fig 2B) in response to serum stimulation and then significantly declined in UASMC ($p < 0.02$ versus peak value; Student's unpaired t -test) to steady-state levels significantly above resting values (Fig 2B); this is also demonstrated by the diphosphorylated band in the Phos-tag gels in Fig 1A and 1C. There was no significant decline in diphosphorylation of LC₂₀ over the 2-h incubation period in CASMC (Fig 2A; $p = 0.13$ versus peak value; Student's unpaired t -test).

Serum-induced phosphorylation of MYPT1

Analysis of MYPT1 phosphorylation at T696 and T853 by western blotting with phosphospecific antibodies revealed a low basal level of phosphorylation at both sites under serum-free conditions in CASMC (Fig 3A and 3B) and UASMC (Fig 3C and 3D). Serum stimulation induced a rapid increase in phosphorylation at both sites in both cell types, which peaked at 1–2 min and declined steadily with time, in most cases returning to basal levels within 2 h of exposure to serum.

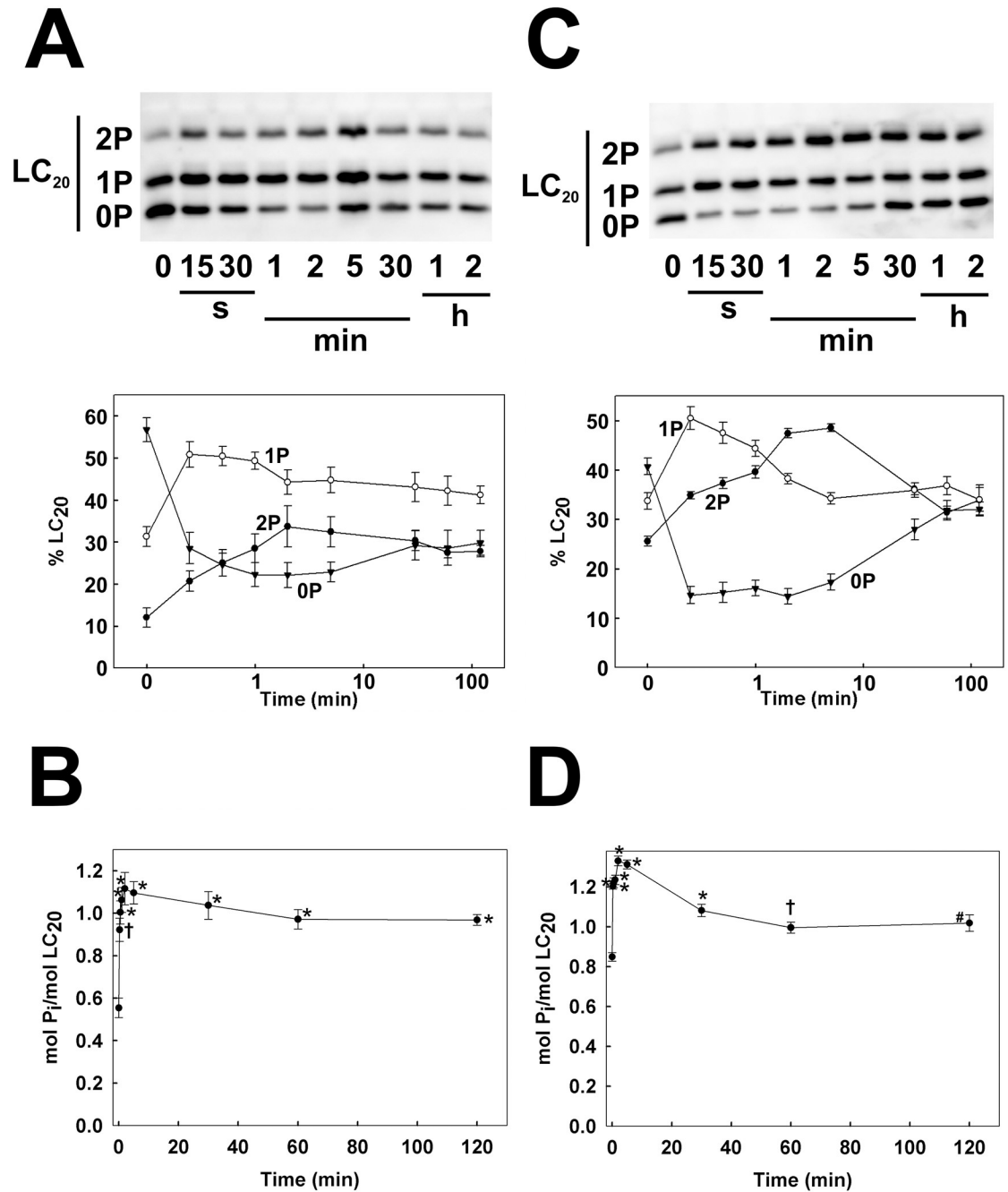


Fig 1. Time courses of serum-induced LC₂₀ phosphorylation in human arterial smooth muscle cells. Human coronary (A, B) and umbilical arterial smooth muscle cells (C, D) were seeded in 4-well plates, serum starved overnight and stimulated with 5% FBS at time zero. Cells were lysed in Laemmli sample buffer at the indicated times of serum stimulation and subjected to Phos-tag SDS-PAGE and western blotting with anti-LC₂₀ to detect unphosphorylated (0P), mono- (1P) and diphosphorylated LC₂₀ (2P). Representative western blots are shown in panels A and C above cumulative quantitative data for each of the LC₂₀ bands. Panels B and D show the time courses of total phosphorylation stoichiometry, calculated as follows: mol P_i/mol LC₂₀ = (1P + 2x2P) / (0P + 1P + 2P). Values indicate the mean ± SEM (n = 7 for panels A and B; n = 6 for panels C and D). Significant differences from the value at time zero are indicated: *p < 0.0001, †p = 0.0001 (B), *p < 0.0001, †p = 0.0023, #p = 0.0004 (D) (Dunnett's *post hoc* test).

<https://doi.org/10.1371/journal.pone.0226406.g001>

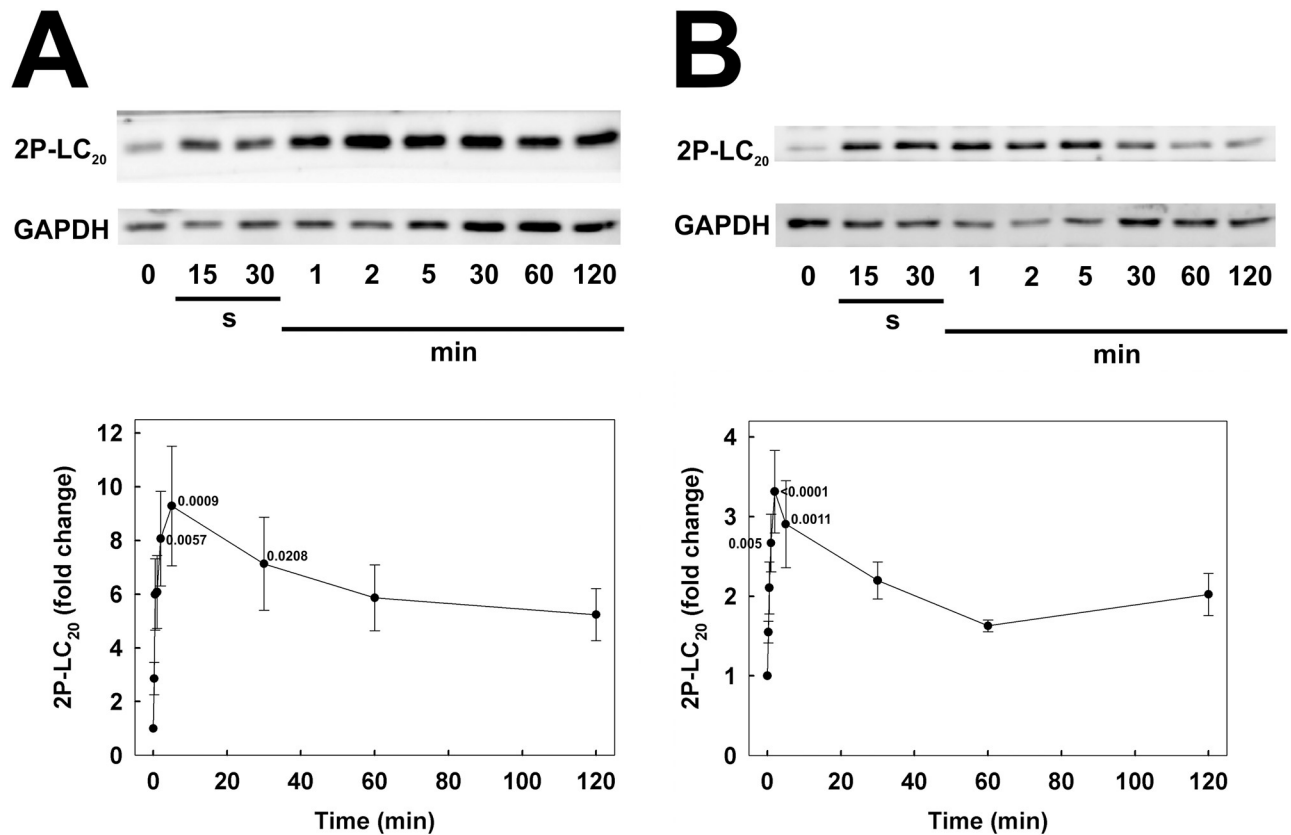


Fig 2. Confirmation of serum-induced LC₂₀ diphosphorylation at T18 and S19. Human coronary (A) and umbilical arterial smooth muscle cells (B) were treated with serum at time zero, as described in the legend to Fig 1, and diphosphorylation of LC₂₀ at T18 and S19 was assessed by regular SDS-PAGE and western blotting with an antibody that specifically recognizes LC₂₀ only when phosphorylated at both T18 and S19. Representative western blots are shown in each panel above cumulative quantitative data depicting the time-dependent changes in LC₂₀ diphosphorylation expressed as fold change relative to the value at time zero (prior to addition of serum) after normalization of loading levels using GAPDH. Values indicate the mean \pm SEM ($n = 6$). Significant differences from the value at time zero are indicated with their respective p values (Dunnett's *post hoc* test).

<https://doi.org/10.1371/journal.pone.0226406.g002>

Serum-induced phosphorylation of Par-4

Analysis of Par-4 phosphorylation at T163 by western blotting with phosphospecific antibodies revealed a low basal level of phosphorylation under serum-free conditions in CASC (Fig 4A) and UASC (Fig 4B). Serum stimulation induced a rapid increase in phosphorylation in both cell types, which peaked at 30 s and declined towards basal levels over the 2-h incubation period.

Serum-induced phosphorylation of Akt

We also investigated the time courses of serum-induced phosphorylation events distinct from the signaling pathways involved in LC₂₀ phosphorylation, specifically the kinases Akt/PKB, ERK1/2 and p38 MAPK as well as the kinase substrate, heat shock protein HSP27. PI3K/Akt signaling in VSMCs is involved in the etiology of atherosclerosis [36,37]. Phosphorylation at T308 and S473 of Akt/PKB is required for full activation [38]. Analysis of Akt phosphorylation at S473 by western blotting with phosphospecific antibodies revealed a low basal level of phosphorylation under serum-free conditions in CASC (S1A Fig) and UASC (S1B Fig). Serum stimulation induced a slower rate of increase in phosphorylation in both cell types compared to the phosphorylation events described above, peaked at 5–30 min and remained elevated over the 2-h incubation period.

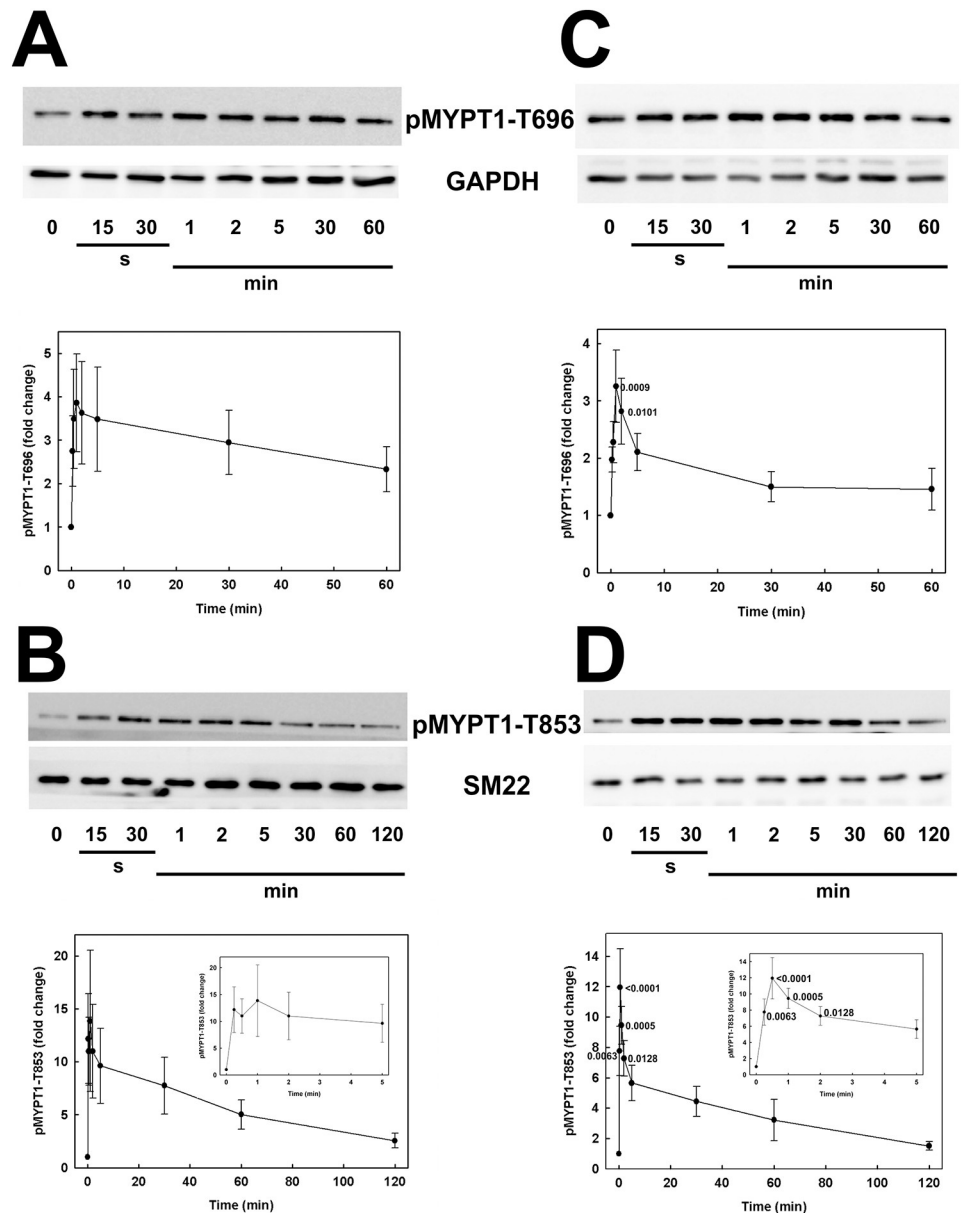


Fig 3. Time courses of serum-induced MYPT1 phosphorylation at T696 and T853 in human arterial smooth muscle cells. Human coronary (A, B) and umbilical arterial smooth muscle cells (C, D) were treated with serum at time zero, as described in the legend to Fig 1. Cells were lysed in Laemmli sample buffer at the indicated times and subjected to SDS-PAGE and western blotting with anti-pT696-MYPT1 (A, C) or anti-pT853-MYPT1 (B, D). Representative western blots are shown in each panel above cumulative quantitative data. Phosphorylated MYPT1 (pMYPT1) signals were normalized to GAPDH (A, C) or SM22 (B, D) and expressed relative to the pMYPT1: GAPDH or pMYPT1: SM22 ratio at time zero. Values indicate the mean \pm SEM ($n = 7$ in A; $n = 8$ in B; $n = 6$ in C and D). Significant differences from the value at time zero are indicated with their respective p values (Dunnett's *post hoc* test). Insets in B and D show the first 5 min of the time courses for greater clarity.

<https://doi.org/10.1371/journal.pone.0226406.g003>

Serum-induced phosphorylation of ERK1/2

The ERK MAPKs, ERK1/p44 and ERK2/p42, are activated by a wide variety of growth factors and mitogens via phosphorylation at the T and Y residues (T202 and Y204 in ERK1 and T185 and Y187 in ERK2) within the activation loop TEY sequence [39]. ERK1 and ERK2 have been implicated in cell migration [40]. Analysis of ERK1 and ERK2 phosphorylation by western

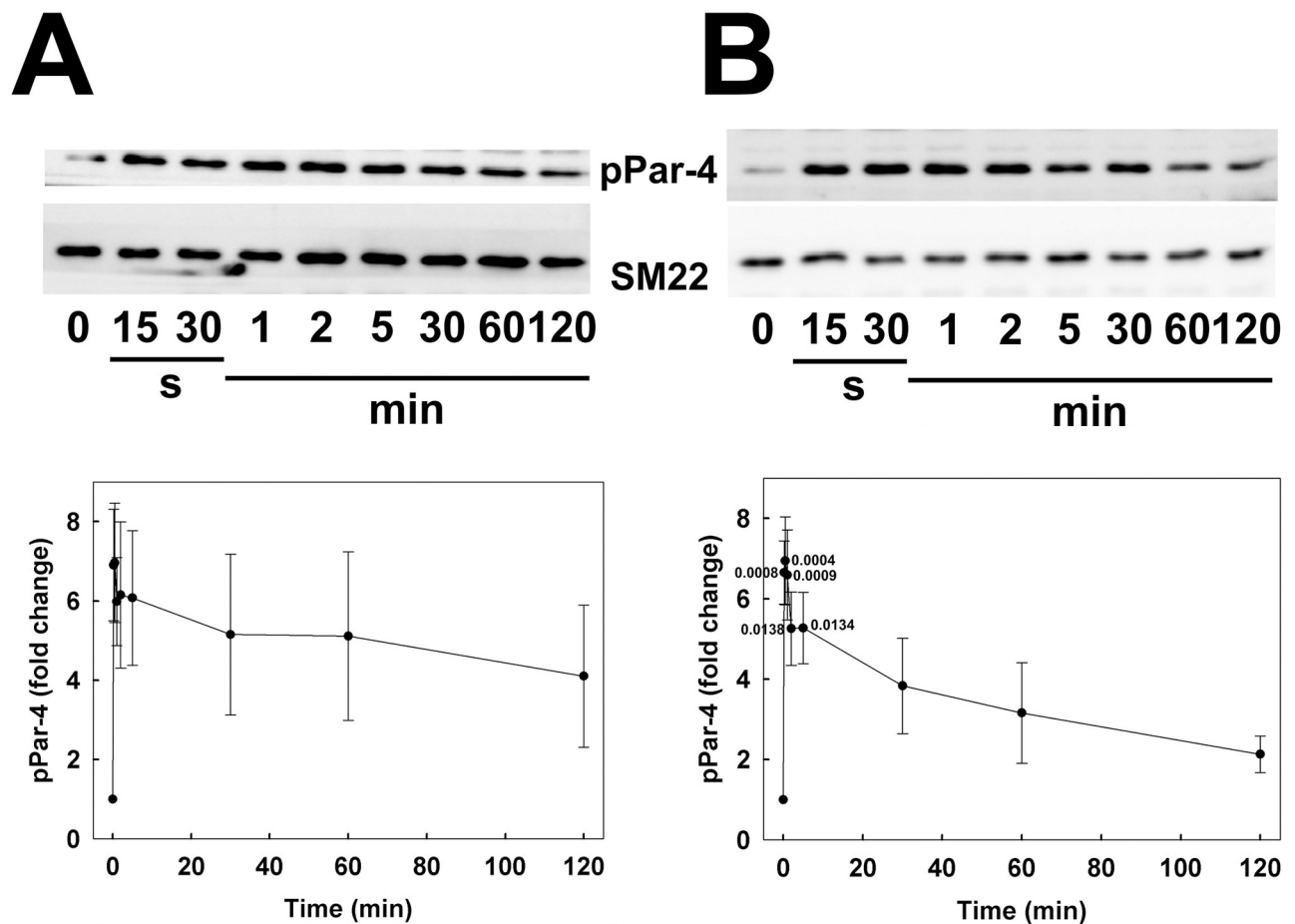


Fig 4. Time courses of serum-induced Par-4 phosphorylation at T163 in human arterial smooth muscle cells. Human coronary (A) and umbilical arterial smooth muscle cells (B) were treated with serum at time zero, as described in the legend to Fig 1. Cells were lysed in Laemmli sample buffer at the indicated times and subjected to SDS-PAGE and western blotting with anti-pT163-Par-4. Representative western blots are shown in each panel above cumulative quantitative data. Phospho-Par-4 signals were normalized to SM22 and expressed relative to the pPar-4: SM22 ratio at time zero. Values indicate the mean \pm SEM ($n = 6$). Significant differences from the value at time zero are indicated with their respective p values (Dunnett's *post hoc* test). The SM22 controls in panels A and B are the same as those in Fig 3B and 3D, respectively, since all three proteins (pMYPT1-T853, pPar-4 and SM22) were analysed on the same gel/blot.

<https://doi.org/10.1371/journal.pone.0226406.g004>

blotting with phosphospecific antibodies revealed a low basal level of phosphorylation under serum-free conditions in CASMC (S2 Fig). Serum stimulation induced a relatively slow increase in phosphorylation of both 44-kDa ERK1 (S2B Fig) and 42-kDa ERK2 (S2C Fig), which peaked at 5 min and remained elevated over the 1-h incubation period. Similar results were observed in UASMC, in which case total ERK phosphorylation was quantified due to the difficulty of achieving clear separation of the two isoforms (S3 Fig).

Serum-induced phosphorylation of p38 MAPK

p38 MAPK has also been implicated in cell migration through activation by several growth factors, cytokines and chemotactic substances [40] and is activated by phosphorylation of the T and Y residues in the TGY motif of the activation loop (T180 and Y182 of human p38MAPK α) [41]. Analysis of p38 MAPK phosphorylation at T180 and Y182 by western blotting with phosphospecific antibodies revealed a low basal level of phosphorylation under serum-free conditions in CASMC (S4A Fig) and UASMC (S4B Fig). Serum stimulation

induced a relatively slow rate of increase in phosphorylation in both cell types, which peaked at 5 min and declined towards basal levels over the 2-h incubation period.

Serum-induced phosphorylation of HSP27

The small heat shock protein HSP27 acts as an ATP-independent chaperone in protein folding, has been implicated in cell migration and cytoskeletal architecture, and is regulated by phosphorylation at multiple sites [42], including S82, which induces polymer assembly and actin binding [43]. Analysis of HSP27 phosphorylation at S82 by western blotting with phosphospecific antibodies revealed a low basal level of phosphorylation under serum-free conditions in CASMC (S4C Fig) and UASMC (S4D Fig). Serum stimulation induced a slow increase in phosphorylation in both cell types, which peaked at 30 min and remained elevated over the 2-h incubation period.

Knockdown of MLCK, ROCK and ZIPK

Transfection with siRNA was used to investigate the involvement of MLCK, ROCK and ZIPK in serum-induced phosphorylation events. Transfection of CASMC with siRNA targeting MLCK reduced MLCK protein to ~55% of control levels (cells transfected with negative control siRNA) but had no effect on ROCK1 or ZIPK levels (Fig 5).

Transfection of CASMC and UASMC with siRNA targeting ROCK1 reduced ROCK1 protein levels to ~27 and ~22% of control (cells transfected with negative control siRNA), respectively (Fig 6), confirming our previous observations [33]. ROCK1-siRNA treatment of CASMC reduced ROCK2 protein levels to ~65% of control (Fig 6B), as we previously reported [33]. On the other hand, ROCK1 knockdown did not significantly affect ZIPK protein (Fig 6): ZIPK levels were ~89 and ~98% of controls in CASMC and UASMC, respectively, consistent with our previous observations [33].

Transfection of CASMC and UASMC with siRNA targeting ZIPK reduced ZIPK protein to ~55% and ~50% of control levels (cells transfected with negative control siRNA), respectively (Fig 6), confirming our previous observations [33]. Consistent with our previous findings [33], ZIPK knockdown was accompanied by an increase in ROCK1 protein to ~165% of control levels in CASMC and to ~133% of control levels in UASMC (Fig 6).

Effect of MLCK knockdown and inhibition on phosphorylation of LC₂₀

To investigate the role of MLCK in LC₂₀ phosphorylation following serum stimulation, we first examined the levels of smooth muscle MLCK in CASMC and UASMC. As shown in Fig 7A, MLCK of the expected molecular weight (130 kDa) for smooth muscle MLCK was clearly detected in CASMC by western blotting, but we could not detect the larger non-muscle isoform of 210 kDa [4]. We were unable to detect a consistent, clear signal for MLCK in UASMC, however, and therefore further experiments were carried out with CASMC. MLCK knockdown had no significant effect on LC₂₀ diphosphorylation at T18 and S19 in response to serum treatment for 2 min, as shown by SDS-PAGE and western blotting with anti-2P-LC₂₀ (Fig 7B). Phos-tag SDS-PAGE and western blotting with anti-LC₂₀ confirmed the lack of effect of MLCK knockdown on serum-induced LC₂₀ phosphorylation: phosphorylation at one and two sites and overall phosphorylation stoichiometry were unaffected by MLCK knockdown (Fig 7C and 7D).

The MLCK inhibitors, ML7 and wortmannin, also had no significant effect on LC₂₀ phosphorylation at T18 and S19 in response to serum treatment. SDS-PAGE and western blotting with anti-2P-LC₂₀ indicated that serum-induced LC₂₀ diphosphorylation was unaffected by ML7 (Fig 8A). Phos-tag SDS-PAGE analysis confirmed that there was no significant difference

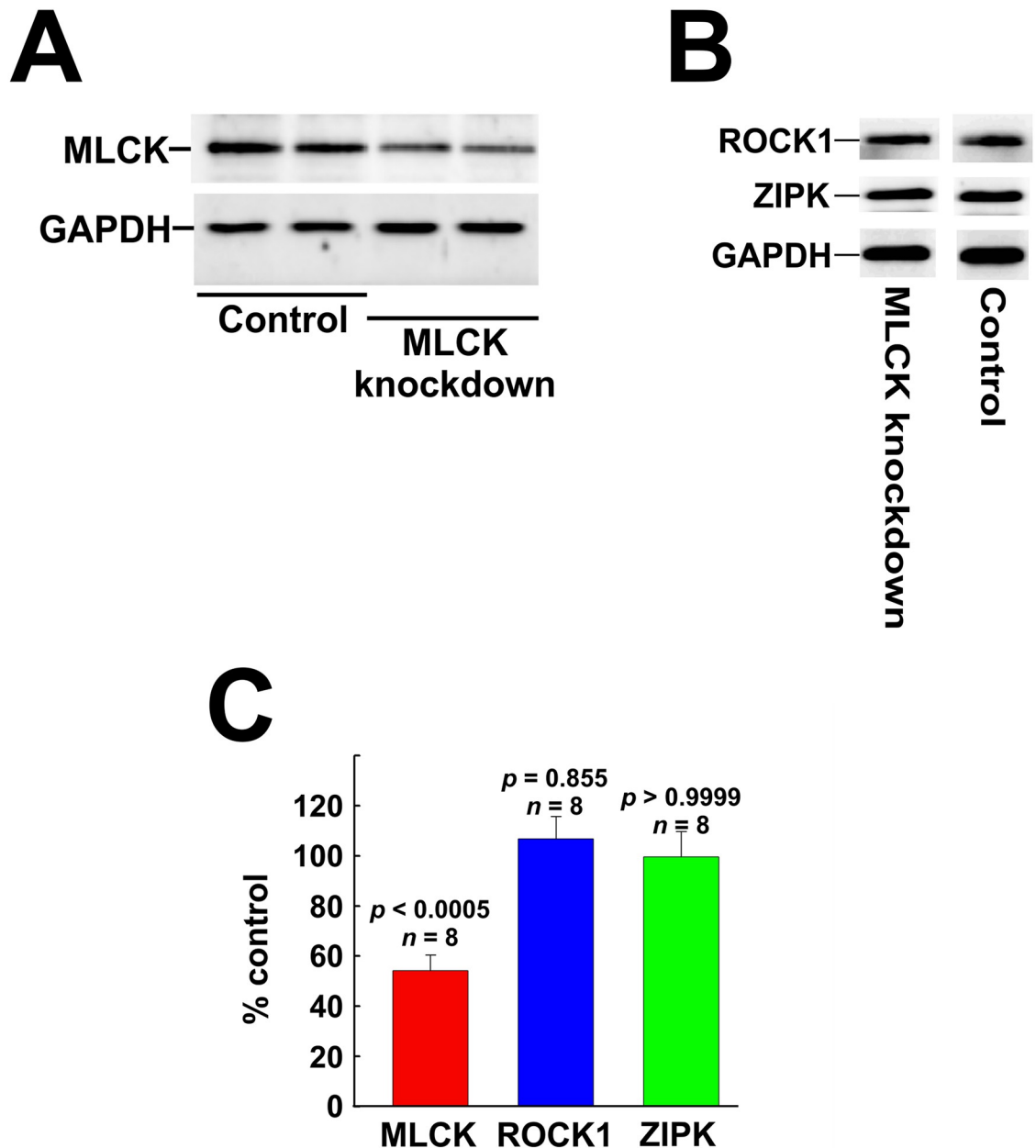


Fig 5. Knockdown of MLCK in cultured coronary arterial smooth muscle cells. MLCK protein was down-regulated in human CASC by siRNA treatment. Controls were treated identically, but with negative control siRNA. (A) Representative western blots of two different knockdown experiments demonstrating siRNA-mediated down-regulation of MLCK. (B) Representative western blots showing the lack of effect of MLCK knockdown on ROCK1 or ZIPK expression in CASC. (C) Quantitative analysis of the effects of MLCK knockdown on MLCK, ROCK1 and ZIPK expression. Statistical analysis was carried out with Dunnett's *post hoc* test.

<https://doi.org/10.1371/journal.pone.0226406.g005>

between serum-induced mono- or diphosphorylation of LC₂₀ in the absence or presence of ML7 (Fig 8B). Likewise, SDS-PAGE and western blotting with anti-2P-LC₂₀ indicated that serum-induced LC₂₀ diphosphorylation was unaffected by wortmannin (Fig 8C), which was confirmed by Phos-tag SDS-PAGE analysis (Fig 8D). In control experiments, we verified the membrane permeability and efficacy of ML7 by demonstrating inhibition of U46619 (thromboxane A₂ mimetic)-induced contraction of de-endothelialized rat caudal arterial smooth

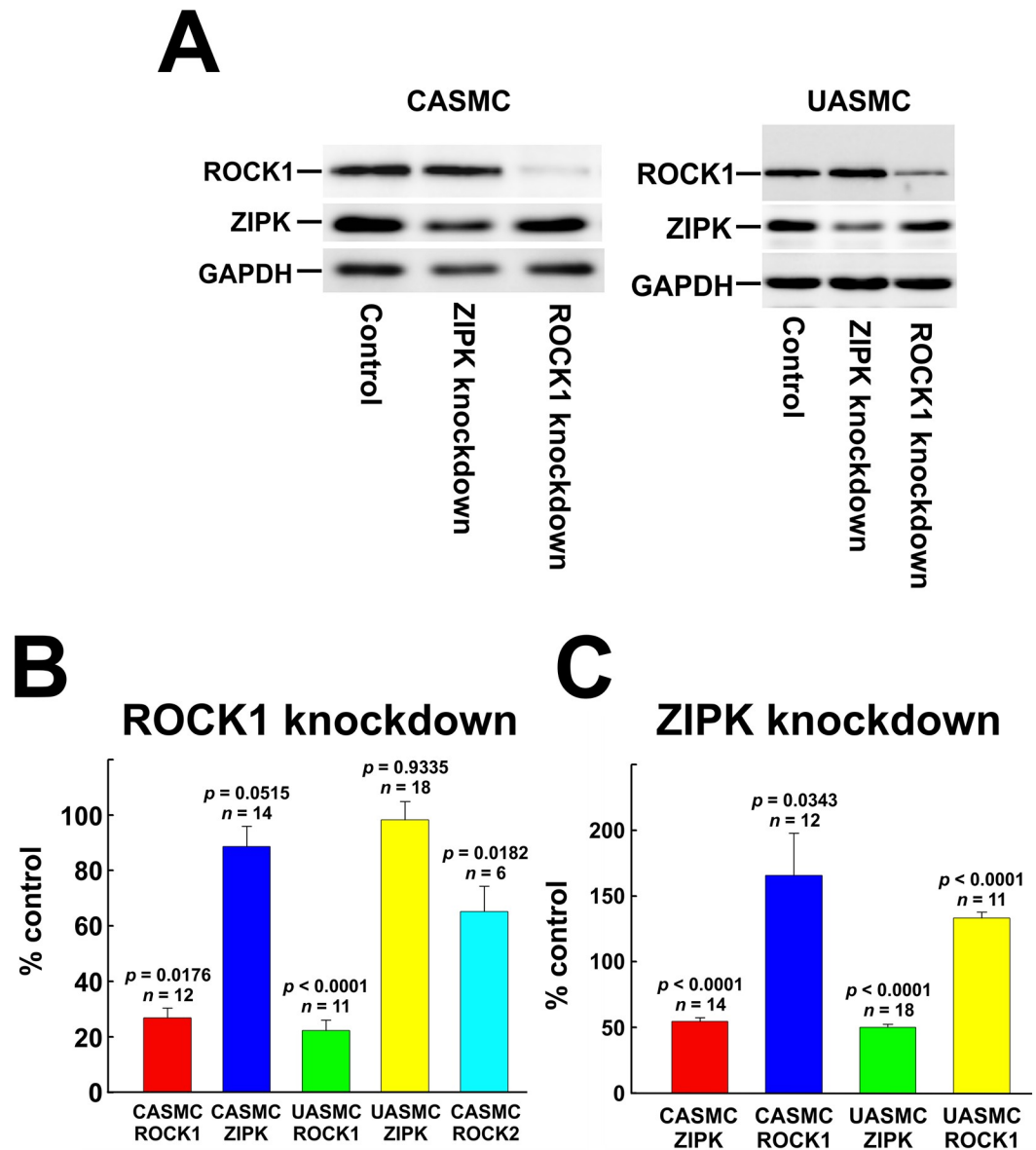


Fig 6. Knockdown of ROCK and ZIPK in cultured vascular smooth muscle cells. (A) Representative western blots showing the effects of ROCK1 or ZIPK knockdown on ROCK1 and ZIPK expression in CASC and UASC. (B) Quantification of ROCK1, ROCK2 and ZIPK levels in ROCK1 siRNA-treated cells compared to controls. (C) Quantification of ROCK1 and ZIPK levels in ZIPK siRNA-treated cells compared to controls. Statistical analysis was carried out with Dunnett's *post hoc* test.

<https://doi.org/10.1371/journal.pone.0226406.g006>

muscle, as described previously [44]. We also verified that wortmannin (an inhibitor of PI 3-kinase as well as MLCK) is membrane permeant and effective since it inhibited phosphorylation of Akt, a PI 3-kinase substrate (S5 Fig).

Finally, chelation of Ca^{2+} with EGTA to remove extracellular Ca^{2+} and deplete intracellular stores had no significant effect on serum-induced LC₂₀ phosphorylation at T18 and S19. From western blotting with anti-diP-LC₂₀, there was no significant difference between the normalized signal intensities for diP-LC₂₀ from cells treated with serum in the presence of Ca^{2+} or EGTA (Fig 9A). From Phos-tag SDS-PAGE and western blotting with anti-LC₂₀, LC₂₀ phosphorylation stoichiometry was identical in the presence of Ca^{2+} and EGTA (Fig 9B). EGTA

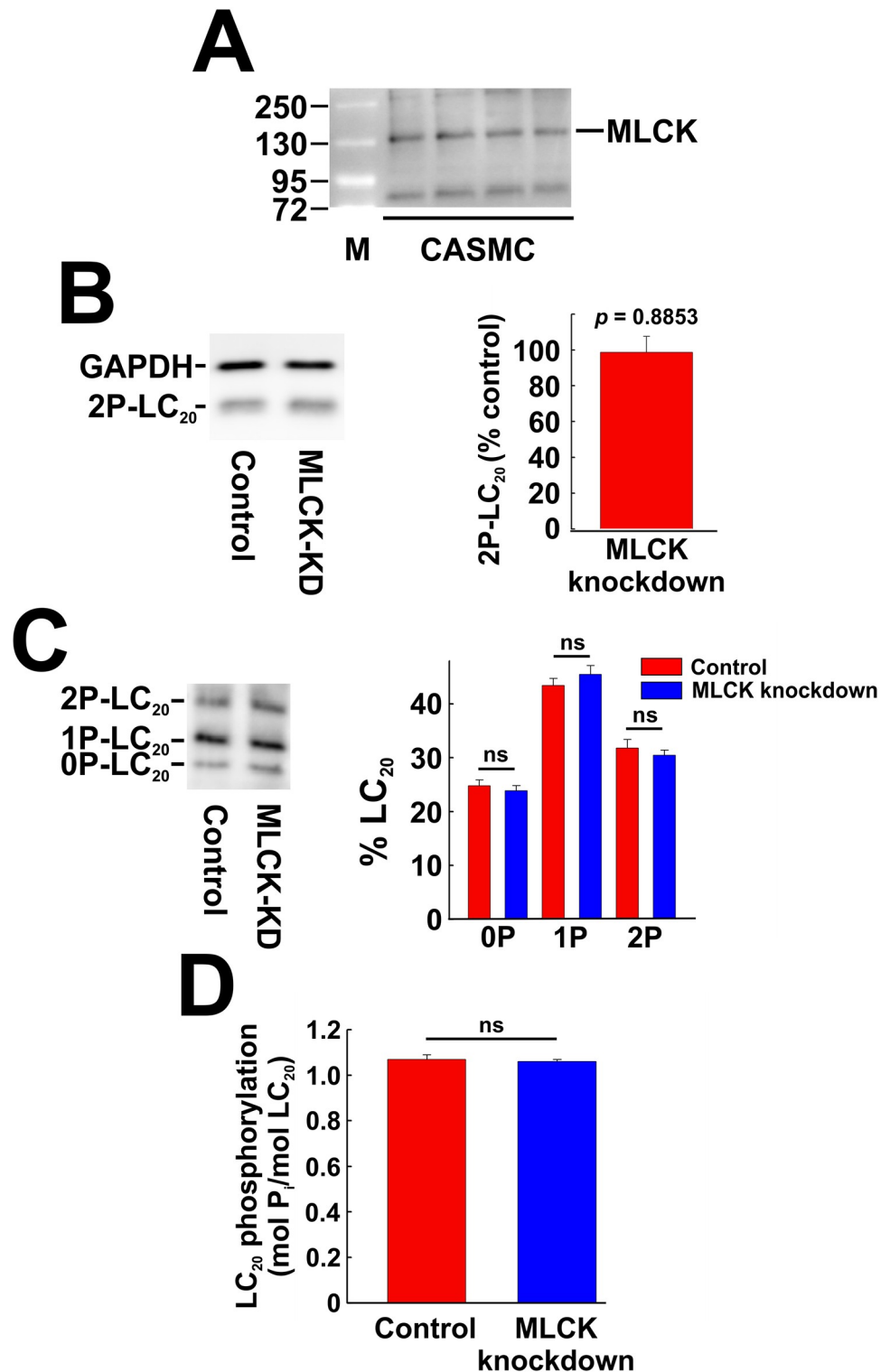


Fig 7. MLCK expression and the effect of knockdown of MLCK on phosphorylation of LC₂₀ in coronary arterial smooth muscle cells. (A) Extracts of CASCMS cultures were subjected to SDS-PAGE and western blotting with anti-MLCK. Lane “M” indicates molecular weight markers. Numbers indicate molecular weights in kDa. (B) Representative western blots with anti-2P-LC₂₀ of extracts of cells treated with negative control siRNA (Control) or siRNA targeting MLCK (MLCK-KD) and then incubated with 5% FBS for 2 min (left-hand panel). GAPDH was used to normalize loading levels. Quantitative data with statistical analysis are provided in the histogram in the right-hand panel ($n = 6$; Student’s unpaired t -test). (C) Phos-tag SDS-PAGE of extracts of cells treated with control or MLCK-targeted siRNA

following 2 min of serum stimulation (left-hand panel). The histogram (right-hand panel) shows quantitative data for unphosphorylated (0P), mono- (1P) and diphosphorylated LC₂₀ (2P). “ns” indicates no significant difference between control and MLCK knockdown cells ($n = 12$; $p > 0.05$; Student’s unpaired t -test). (D) Quantification of LC₂₀ phosphorylation stoichiometry confirmed that there was no significant effect of MLCK knockdown on serum-induced LC₂₀ phosphorylation ($n = 12$; $p = 0.9918$; Student’s unpaired t -test).

<https://doi.org/10.1371/journal.pone.0226406.g007>

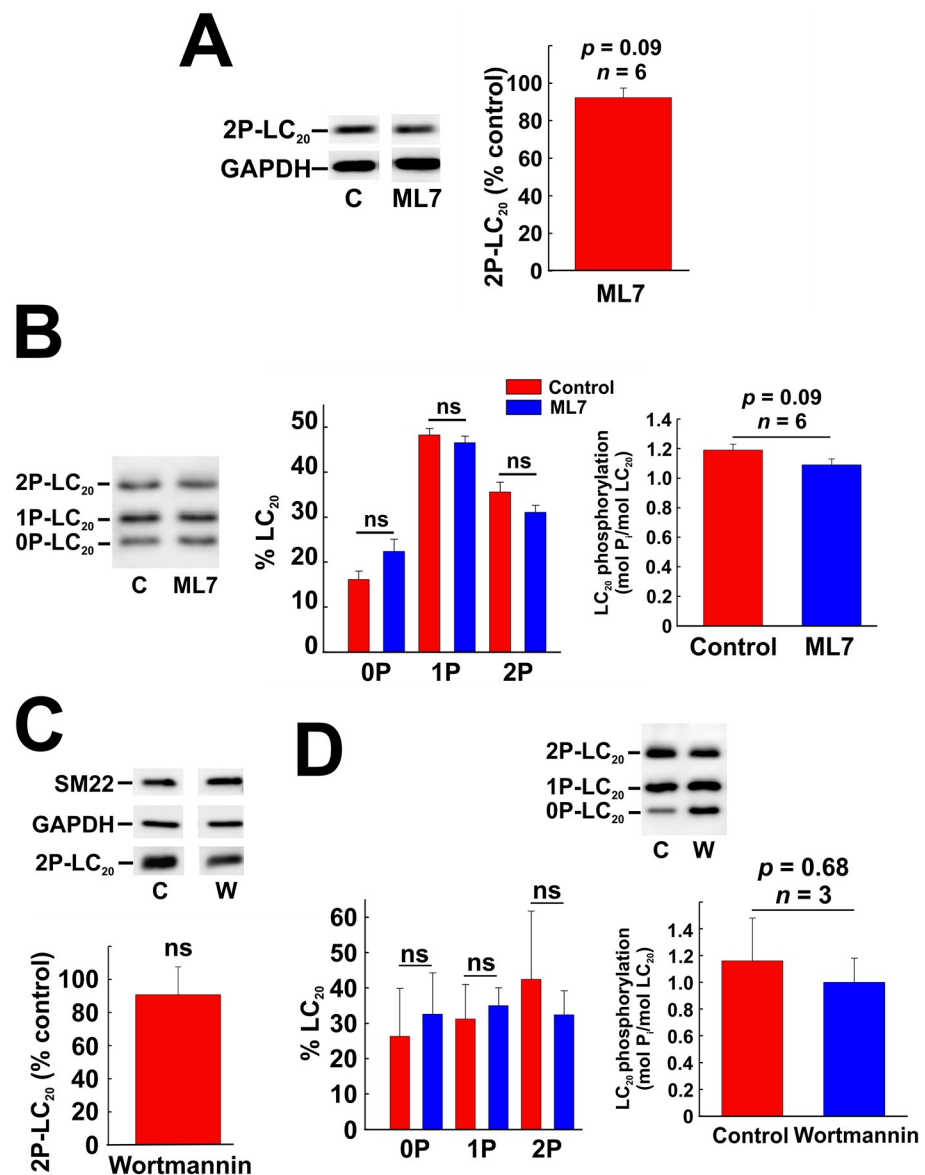
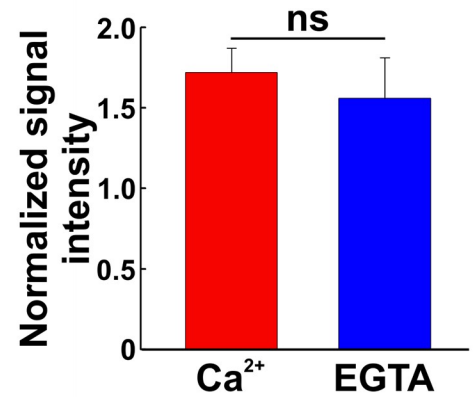
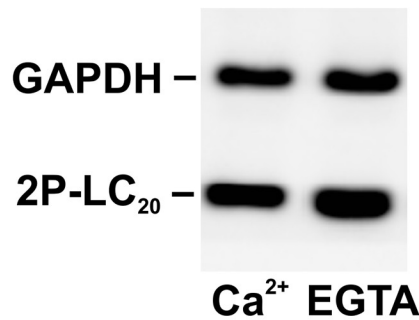


Fig 8. Effect of inhibition of MLCK on phosphorylation of LC₂₀ in coronary arterial smooth muscle cells. (A) Effect of ML7 (10 μ M) pre-treatment on serum-induced LC₂₀ diphosphorylation (analysed by western blotting with anti-2P-LC₂₀; left-hand panel) with quantitative analysis (right-hand panel). Statistical analysis was carried out with Student’s unpaired t -test. (B) Effect of ML7 (10 μ M) pre-treatment on LC₂₀ phosphorylation (analysed by Phos-tag SDS-PAGE and western blotting with anti-LC₂₀) following 2 min of serum stimulation. Controls (C) were incubated with vehicle rather than ML7. A representative western blot is shown in the left-hand panel, quantification of unphosphorylated, mono- and diphosphorylated LC₂₀ in the middle panel and overall phosphorylation stoichiometry in the right-hand panel ($n = 6$). Statistical analysis was carried out with Student’s unpaired t -test. (C) Effect of wortmannin (1 μ M) pre-treatment on serum-induced LC₂₀ diphosphorylation (analysed by western blotting with anti-2P-LC₂₀; upper panel) with quantitative analysis ($n = 3$; lower panel). (D) Effect of wortmannin (1 μ M) pre-treatment on serum-induced LC₂₀ diphosphorylation (analysed by Phos-tag SDS-PAGE with anti-LC₂₀; upper panel) with quantitative analysis (lower panels). “ns” denotes $p > 0.05$ (Student’s unpaired t -test).

<https://doi.org/10.1371/journal.pone.0226406.g008>

A



B

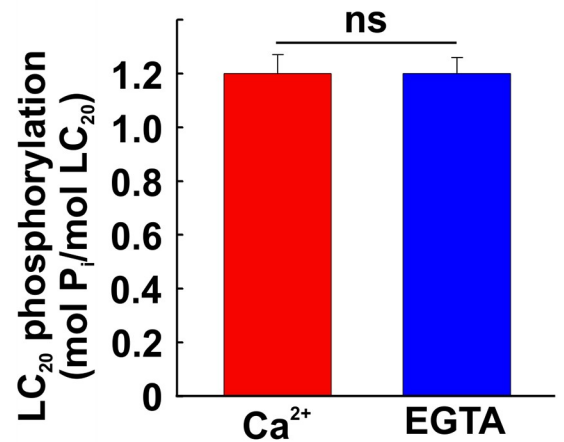
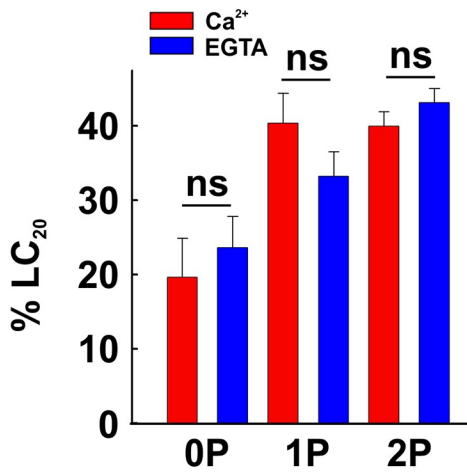
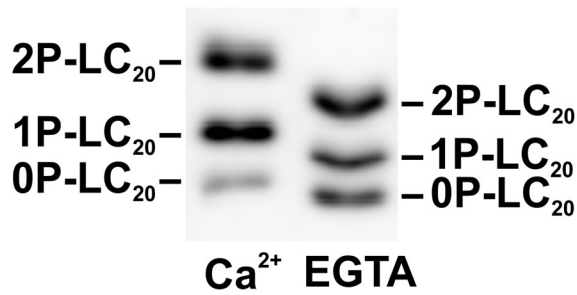


Fig 9. Effect of EGTA treatment on serum-induced LC₂₀ phosphorylation. CASMC were incubated in medium containing Ca²⁺ (2.5 mM) or EGTA (5 mM) and treated with serum for 2 min prior to SDS-PAGE and western blotting with anti-2P-LC₂₀ (A; left-hand panel) or Phos-tag SDS-PAGE and western blotting with anti-LC₂₀ (B; upper panel). Quantitative data are depicted in the corresponding histograms in panels A and B (*n* = 3 in panel A and *n* = 6 in panel B). "ns" denotes *p* > 0.05 (Student's unpaired *t*-test).

<https://doi.org/10.1371/journal.pone.0226406.g009>

treatment affected the mobility of LC₂₀ species during Phos-tag SDS-PAGE (Fig 9B) but did not affect the phosphorylation stoichiometry. We are confident that the high concentration of EGTA used (5 mM) does effectively deplete the endogenous calcium stores in smooth muscle cells since we have shown that a lower EGTA concentration (2 mM) abolished both caffeine-induced and U-46619-induced contraction of de-endothelialized rat caudal arterial smooth muscle and U-46619-induced LC₂₀ phosphorylation, which occurred exclusively at S19 [44].

Effect of ROCK knockdown on phosphorylation of LC₂₀, MYPT1 and Par-4

ROCK-knockdown and control cells were serum starved overnight, treated with 5% FBS for 2 min and lysed for SDS-PAGE and western blotting. Down-regulation of ROCK correlated with significant reductions in serum-induced diphosphorylation of LC₂₀ (Fig 10), of MYPT1 at T696 and T853, and of Par-4 at T163 in both CASMC and UASMC (Fig 11).

Effect of ROCK inhibition on phosphorylation of LC₂₀, MYPT1 and Par-4

Pre-treatment of cells with the ROCK inhibitor GSK429286A (1 μM) had a pronounced inhibitory effect on serum-induced LC₂₀ diphosphorylation in both CASMC and UASMC (Fig 12A and 12D). Phos-tag SDS-PAGE confirmed that LC₂₀ phosphorylation stoichiometry was reduced by ROCK inhibition in CASMC and UASMC (Fig 13A and 13B). ROCK inhibition by GSK429286A also markedly reduced the serum-induced increase in phosphorylation of MYPT1 at T853 and of Par-4 at T163, but had no significant inhibitory effect on MYPT1 phosphorylation at T696 (Fig 12A and 12D). Similarly, ROCK inhibition by H1152 (0.2 μM) in CASMC had no effect on MYPT1 phosphorylation at T696 but markedly reduced MYPT1 phosphorylation at T853 and Par-4 phosphorylation at T163 (Fig 12B, 12C and 12D).

Effect of ZIPK knockdown on phosphorylation of LC₂₀, MYPT1 and Par-4

ZIPK-knockdown and control cells were serum starved overnight, treated with 5% FBS for 2 min and lysed for SDS-PAGE and western blotting. LC₂₀ diphosphorylation was reduced to ~60% of control in CASMC and UASMC (Fig 11A, 11B and 11D). Phos-tag SDS-PAGE confirmed that ZIPK knockdown caused a small, but significant reduction in serum-induced LC₂₀ phosphorylation in both CASMC and UASMC (Fig 10). ZIPK knockdown in both CASMC and UASMC increased MYPT1 phosphorylation at T696 and T853 and Par-4 phosphorylation at T163 (Fig 11A, 11B and 11D). The increases in MYPT1 and Par-4 phosphorylation could be accounted for by the increase in ROCK protein levels induced by ZIPK knockdown shown earlier (Fig 6).

Effect of ZIPK inhibition on phosphorylation of LC₂₀, MYPT1 and Par-4

ZIPK inhibition by HS38 [28] attenuated the increase in LC₂₀ diphosphorylation induced by treatment of CASMC and UASMC with 5% FBS for 2 min, but had no effect on the phosphorylation of MYPT1 at T696 or T853 or of Par-4 at T163 (Fig 12A and 12E). Phos-tag SDS-PAGE confirmed that HS38 reduced the serum-induced phosphorylation stoichiometry of LC₂₀ in CASMC and UASMC (Fig 13A and 13C).

Serum-induced phosphorylation of ZIPK and the effect of ROCK and ZIPK knockdown and inhibition

ZIPK phosphorylation, reflecting activation of the kinase [45], was assessed by Phos-tag SDS-PAGE to separate phosphorylated and unphosphorylated forms of the enzyme, which were then detected by western blotting with a pan-ZIPK antibody. Under serum-free

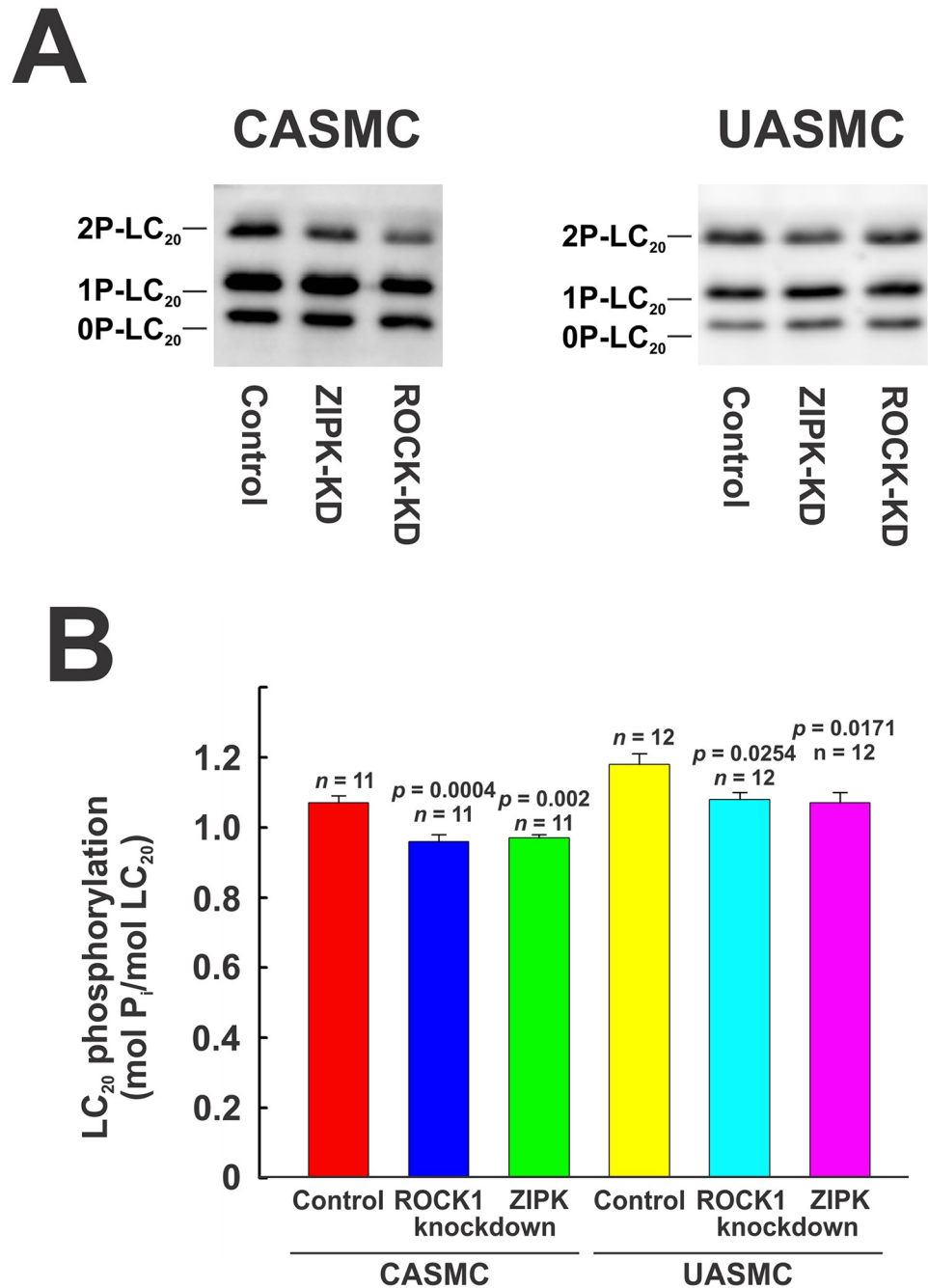


Fig 10. Effect of knockdown of ROCK1 or ZIPK on phosphorylation of LC₂₀ in human arterial smooth muscle cells assessed by Phos-tag SDS-PAGE. ROCK1 or ZIPK was down-regulated in CASMC and UASMC by siRNA treatment. Controls were treated identically, but with negative control siRNA. Cells were serum starved overnight and treated with 5% FBS for 2 min prior to lysis in Laemmli sample buffer for Phos-tag SDS-PAGE and western blotting with anti-LC₂₀. Representative western blots are shown in panel A (CASMC and UASMC) and cumulative quantitative data are provided in the histograms in panel B. Data in panel B are presented as LC₂₀ phosphorylation stoichiometry and values represent the mean ± SEM with the indicated *p* and *n* values with *p* < 0.05 considered statistically significant (Dunnett's *post hoc* test).

<https://doi.org/10.1371/journal.pone.0226406.g010>

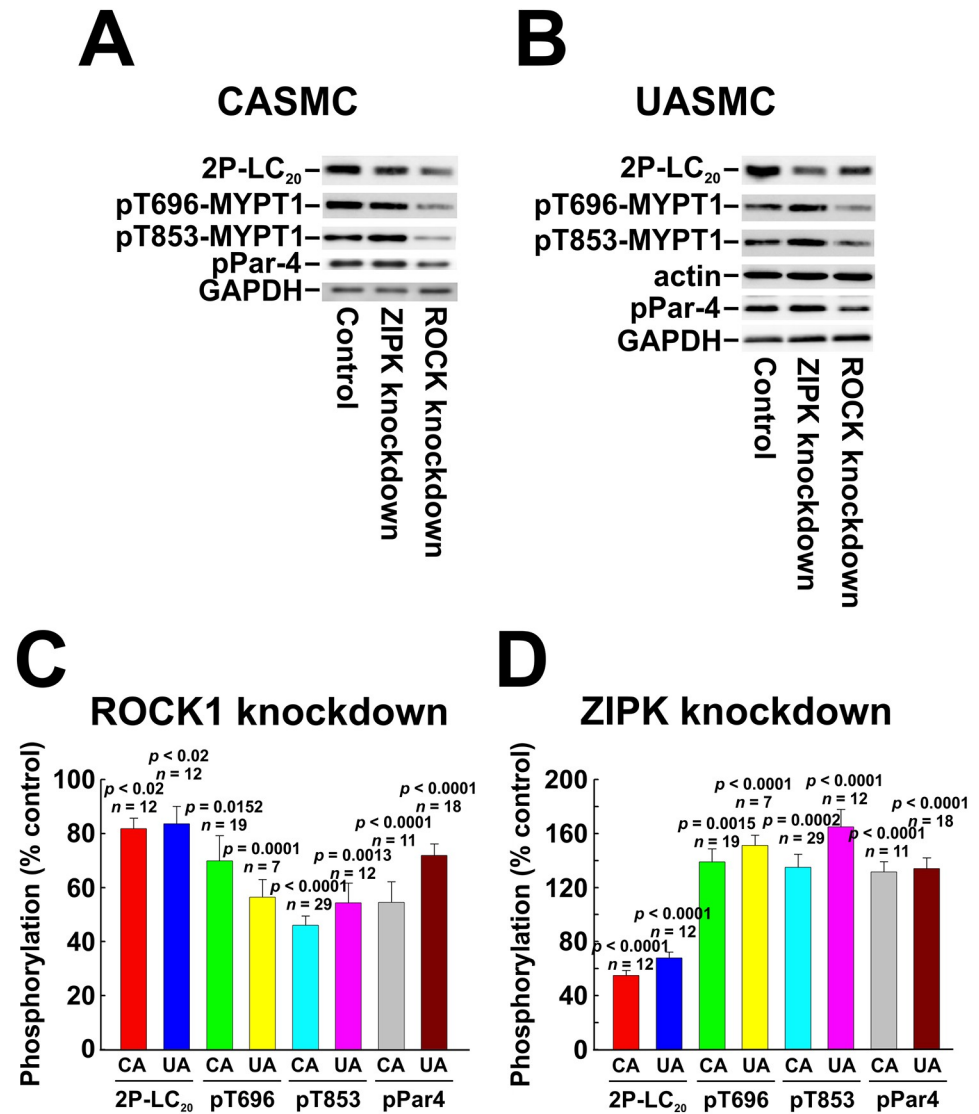


Fig 11. Effect of knockdown of ROCK1 or ZIPK on phosphorylation of LC₂₀, MYPT1 and Par-4 in human arterial smooth muscle cells. ROCK1 or ZIPK was down-regulated in CASMC and UASMC by siRNA treatment. Controls were treated identically, but with negative control siRNA. Cells were serum starved overnight and treated with 5% FBS for 2 min prior to lysis in Laemmli sample buffer for SDS-PAGE and western blotting. GAPDH and actin were used as loading controls; each control shown is for the blot(s) above it. Representative western blots are shown in panels A (CASMC) and B (UASMC) and cumulative quantitative data are provided in the histograms (C, D). Data in panels C and D are presented as % control and values represent the mean ± SEM with the indicated *p* and *n* values with *p* < 0.05 considered statistically significant (Dunnett's *post hoc* test).

<https://doi.org/10.1371/journal.pone.0226406.g011>

conditions, ZIPK was partially phosphorylated in CASMC and UASMC with low levels of phosphorylation at one, two, three and four sites (time zero samples in Fig 14A and 14B, respectively). Serum treatment induced a rapid increase in ZIPK phosphorylation, particularly of the diphosphorylated protein, which was maintained for ≥ 1 h in CASMC (Fig 14A) but transient in UASMC (Fig 14B). Knockdown of ROCK1 had a significant inhibitory effect on serum-induced ZIPK phosphorylation, while ZIPK siRNA treatment reduced ZIPK levels but did not affect the protein's phosphorylation in response to serum treatment (Fig 15A, left-hand panel). Chelation of divalent cations with EDTA resulted in a single band of ZIPK

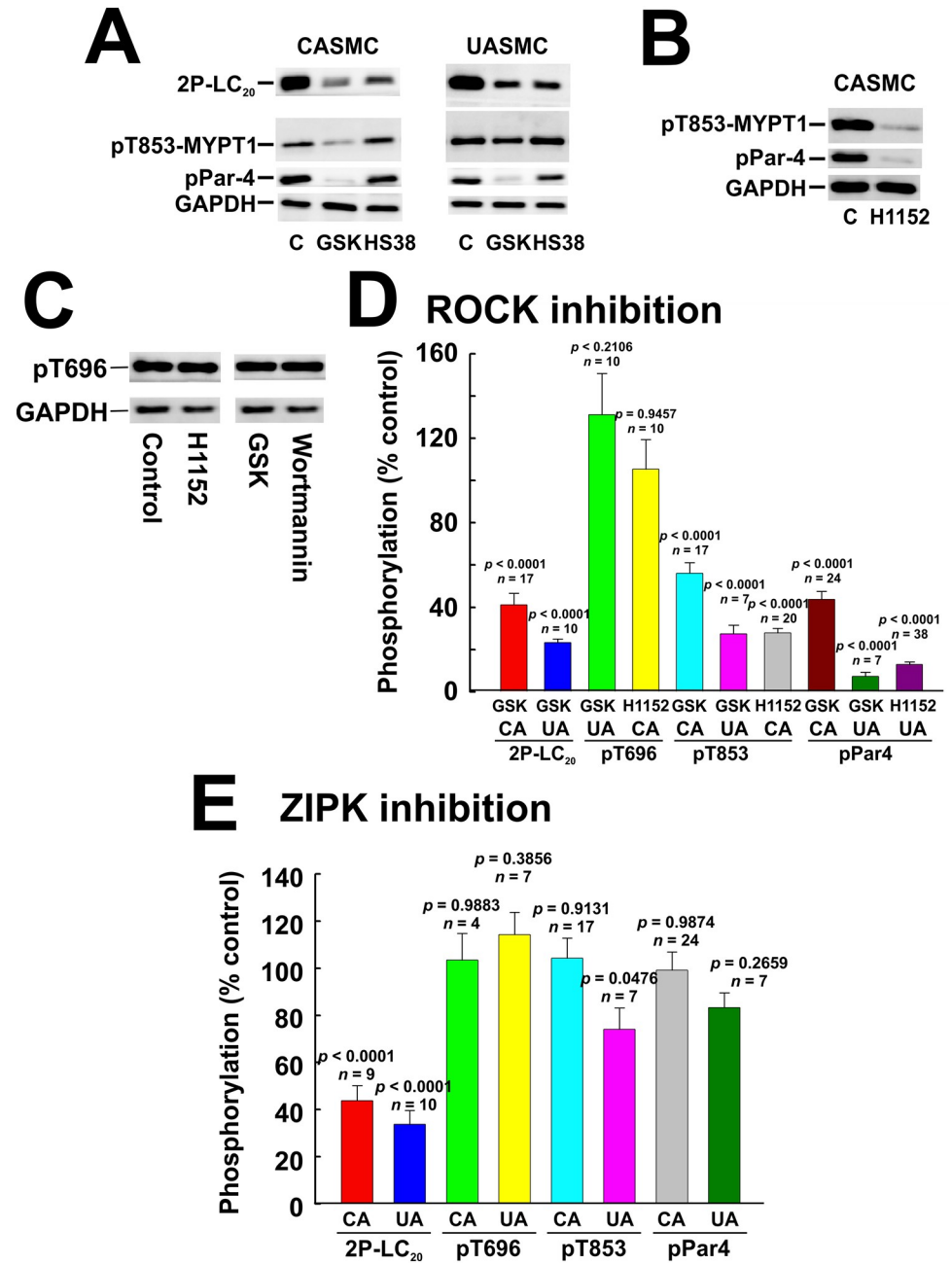


Fig 12. Effect of inhibition of ROCK or ZIPK on phosphorylation of LC₂₀, MYPT1 and Par-4 in human arterial smooth muscle cells. CASMC or UASMC were serum starved overnight, incubated for 40 min with GSK429286A (GSK; 1 μ M), HS38 (10 μ M), H1152 (1 μ M) or vehicle control (C) and treated with 5% FBS for 2 min prior to lysis in Laemmli sample buffer for SDS-PAGE and western blotting with anti-2P-LC₂₀, anti-pT853-MYPT1 or anti-pT163-Par-4 (A), with anti-pT853-MYPT1 or anti-pT163-Par-4 (B) or with anti-pT696-MYPT1 (C). Phosphorylated bands were quantified by scanning densitometry and normalized to the loading control (GAPDH). (D, E) Quantitative data showing the effects of ROCK inhibition with GSK429286A or H1152 (D) or ZIPK inhibition with HS38 (E) on serum-induced phosphorylation of the indicated proteins. Data are presented as % control and values represent the mean \pm SEM with the indicated p and n values with $p < 0.05$ considered statistically significant (Dunnett's *post hoc* test).

<https://doi.org/10.1371/journal.pone.0226406.g012>

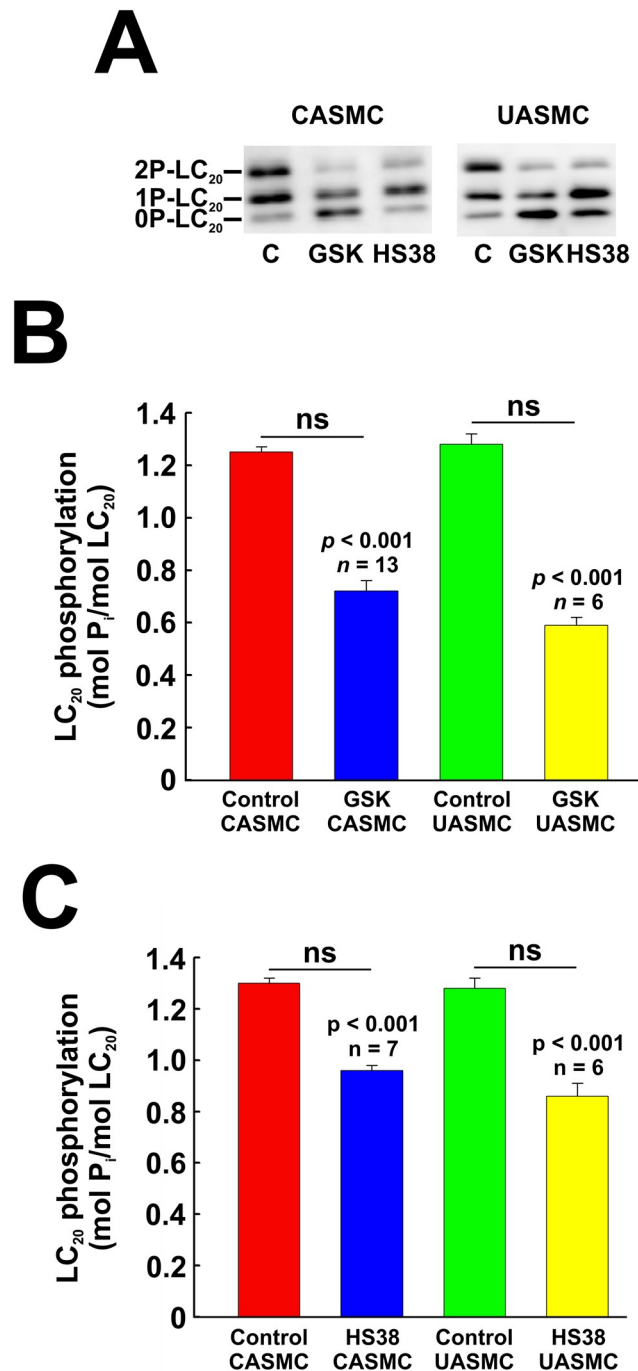


Fig 13. Effect of inhibition of ROCK or ZIPK on phosphorylation of LC₂₀ assessed by Phos-tag SDS-PAGE. CASMC or UASMC were serum starved overnight, incubated for 40 min with GSK429286A (GSK; 1 μM), HS38 (10 μM) or vehicle control (C) and treated with 5% FBS for 2 min prior to lysis in Laemmli sample buffer for Phos-tag SDS-PAGE and western blotting with anti-LC₂₀ (A). (B, C) Unphosphorylated (0P-LC₂₀), monophosphorylated (1P-LC₂₀) and diphosphorylated LC₂₀ (2P-LC₂₀) bands were quantified by scanning densitometry. Data are presented as LC₂₀ phosphorylation stoichiometry and values represent the mean ± SEM with the indicated *p* and *n* values with *p* < 0.05 considered statistically significant (Dunnett's *post hoc* test).

<https://doi.org/10.1371/journal.pone.0226406.g013>

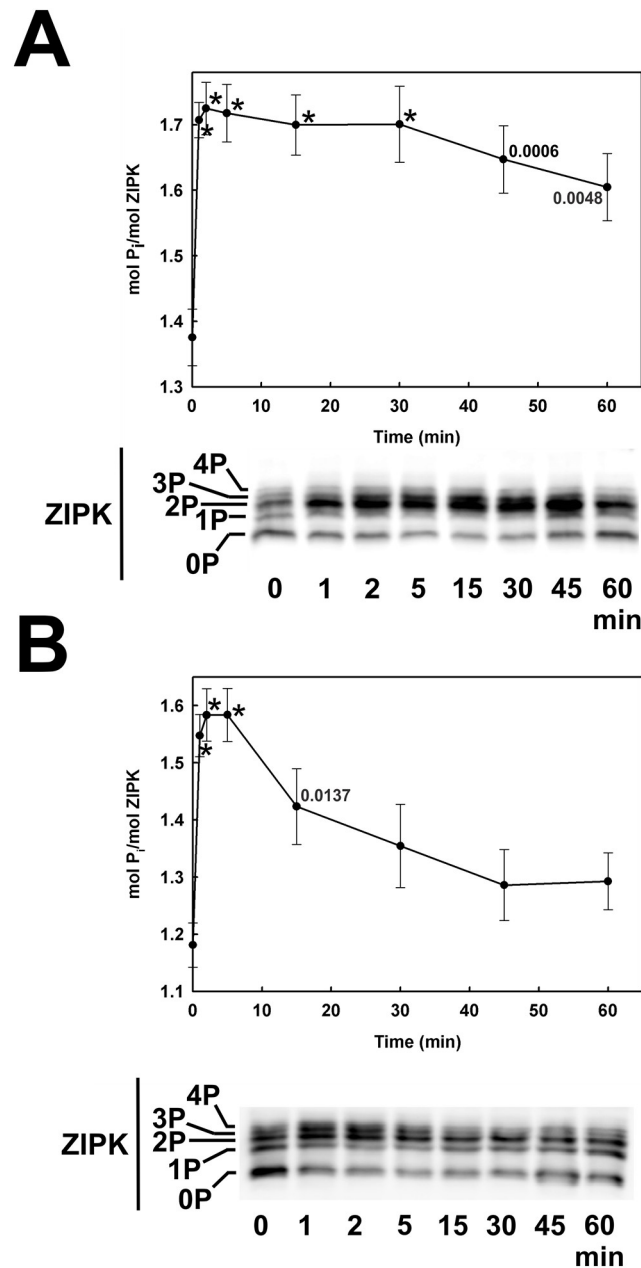


Fig 14. Time courses of serum-induced ZIPK phosphorylation in human arterial smooth muscle cells. Human coronary (A) and umbilical arterial smooth muscle cells (B) were treated with serum at time zero, as described in the legend to Fig 1. Cells were lysed in Laemmli sample buffer at the indicated times and subjected to Phos-tag SDS-PAGE and western blotting with anti-ZIPK as described in the Materials and Methods section. Representative western blots are shown below the time courses of ZIPK phosphorylation stoichiometry. Data are presented as mean \pm SEM ($n = 9$ in panel A; $n = 11$ in panel B). Statistically significant differences from ZIPK phosphorylation stoichiometry at time zero are denoted by * ($p < 0.0001$) or by the actual p values (Dunnett's *post hoc* test).

<https://doi.org/10.1371/journal.pone.0226406.g014>

corresponding to the migration of the unphosphorylated protein (Fig 15A, right-hand panel) confirming that the slower migrating bands observed in the presence of MnCl₂ (Fig 15A, left-hand panel) are indeed phosphorylated forms of ZIPK. Inhibitors of ROCK (GSK429286A) and ZIPK (HS38) inhibited the serum-induced phosphorylation of ZIPK in CASMC (Fig 15B)

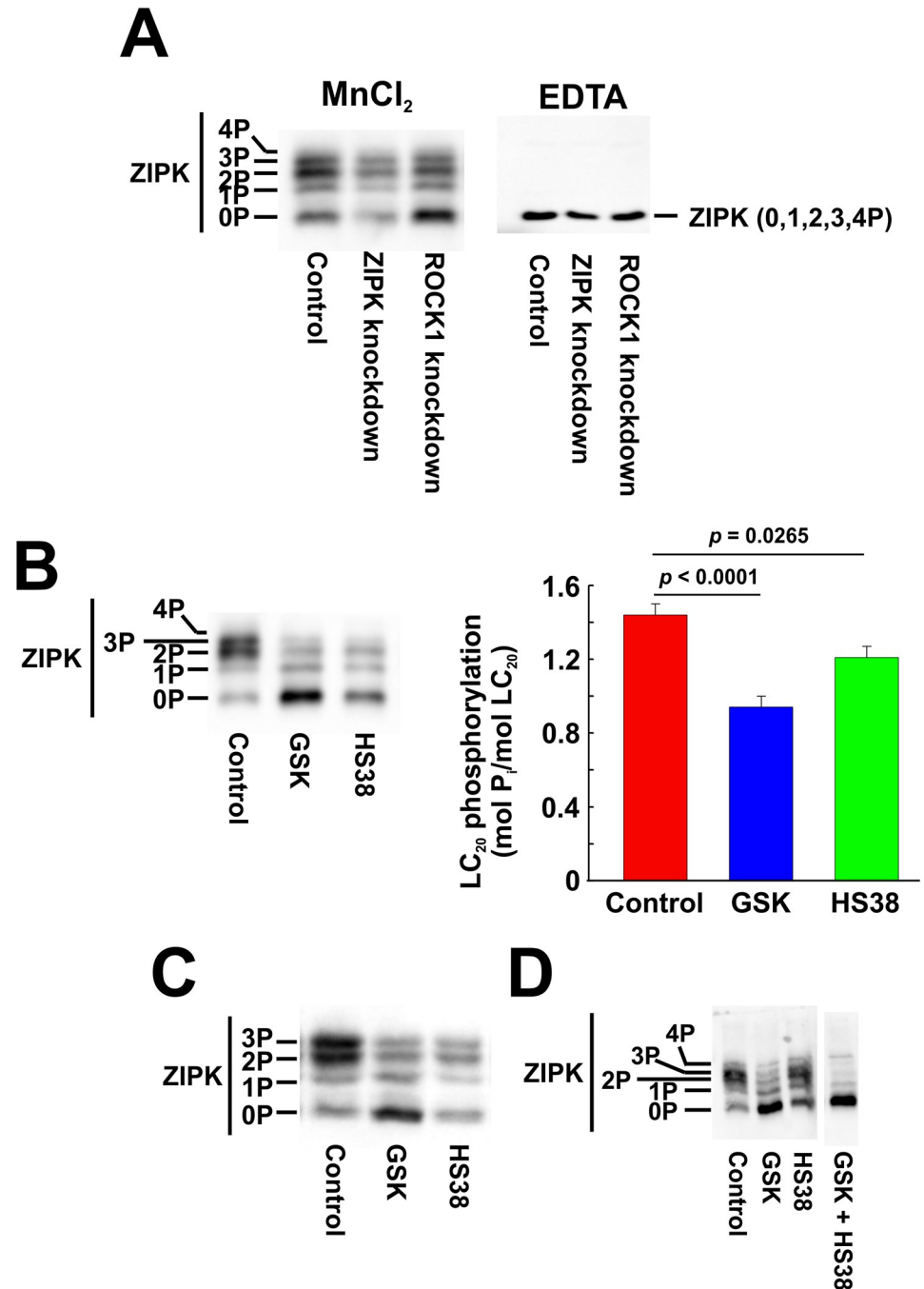


Fig 15. Effect of ROCK1 and ZIPK knockdown and inhibition on serum-induced ZIPK phosphorylation. (A) ROCK1 or ZIPK expression was down-regulated in CASMC by siRNA treatment. Controls were treated identically, but with negative control siRNA. Cells were serum starved overnight and treated with 5% FBS for 2 min prior to lysis in Laemmli sample buffer for Phos-tag SDS-PAGE and western blotting with anti-ZIPK. Electrophoresis was carried out in the presence of MnCl₂ or EDTA as indicated. CASMC (B) or UASMC (C) were serum starved overnight and treated with 5% FBS for 2 min in the absence (control) or presence of GSK429286A (GSK; 1 μM) or HS38 (10 μM) prior to lysis in Laemmli sample buffer for Phos-tag SDS-PAGE and western blotting with anti-ZIPK. Representative blots are shown (n = 11 in panel A; n = 7 in panel B; n = 4 in panel C; n = 3 in panel D). Statistically significant differences in LC₂₀ phosphorylation stoichiometry from control are denoted by the actual p values (Dunnett's *post hoc* test; panel B).

<https://doi.org/10.1371/journal.pone.0226406.g015>

and UASMC (Fig 15C) suggesting that ROCK phosphorylates ZIPK, and ZIPK can autophosphorylate. The combination of ROCK and ZIPK inhibitors prevented ZIPK phosphorylation induced by serum stimulation and almost abolished the basal level of ZIPK phosphorylation in the absence of serum stimulation of UASMC (Fig 15D).

Effects of kinase knockdown and inhibition on LC₂₀ phosphorylation under serum-free conditions

As shown in Fig 1, there is a basal level of LC₂₀ diphosphorylation in serum-starved cultured human vascular smooth muscle cells. We used a combination of siRNA-mediated knockdown and pharmacological inhibition to evaluate the roles of MLCK, ROCK and ZIPK in the regulation of LC₂₀ phosphorylation in the absence of serum stimulation. Phos-tag SDS-PAGE and western blotting with anti-LC₂₀ showed no effect of MLCK knockdown on LC₂₀ phosphorylation under serum-free conditions (Fig 16A). The MLCK inhibitors, ML7 and wortmannin, also had no significant effect on LC₂₀ phosphorylation at T18 and S19 under serum-free conditions (Fig 16B and 16C, respectively). Furthermore, chelation of Ca²⁺ with EGTA had no effect on LC₂₀ phosphorylation at T18 and S19 in the absence of serum stimulation (Fig 16D). Finally, ROCK1 knockdown (Fig 17A) or inhibition by GSK429286A (Fig 17B) or ZIPK knockdown (Fig 17A) or inhibition with HS38 (Fig 17B) under serum-free conditions did not have a significant effect on LC₂₀ phosphorylation under serum-free conditions.

Discussion

The contractile response of smooth muscle can be enhanced or sustained by the process of Ca²⁺ sensitization, which involves a reduction in MLCP activity leading to an increase in the MLCK: MLCP activity ratio [46,47] and sometimes involves diphosphorylation of LC₂₀ at T18 and S19 [9]. Similar findings have been reported in cultured smooth muscle and non-muscle cells [11–13]. In this study, we focused on two protein kinases, ROCK [48,49] and ZIPK [50–52], that have been implicated in the process of Ca²⁺ sensitization and LC₂₀ diphosphorylation [15,18,20,53–55]. Furthermore, while LC₂₀ is unlikely to be a direct physiological substrate of ROCK in smooth muscle tissue [56–62], there is evidence of direct phosphorylation of LC₂₀ at T18 and S19 by ROCK in cultured cells [63,64]. Likewise, ZIPK has been shown to phosphorylate LC₂₀ at both T18 and S19 [18–20,55]. Both kinases are Ca⁺-independent, unlike MLCK which requires Ca²⁺/calmodulin for activity and phosphorylates LC₂₀ exclusively at S19 [9].

ROCK has been shown to phosphorylate the myosin targeting subunit of MLCP (MYPT1) at T696 and T853 (human MYPT1 numbering; GenBank ID number: 289142212) resulting in decreased phosphatase activity [46,48,65–70]. T696 can be phosphorylated by several other protein kinases [54,69] and it appears to be constitutively phosphorylated, i.e. significantly phosphorylated in the absence of stimulation [71]. T853 is more commonly phosphorylated in response to stimulation [44,71]. ROCK can also phosphorylate Par-4 at T163, which abolishes the interaction of Par-4 with MYPT1 and exposes T696 and T853 of MYPT1 to endogenous kinases, resulting in inhibition of MLCP activity, increased LC₂₀ phosphorylation and contraction [72]. While this regulatory mechanism was demonstrated in cultured cells, its operation in vascular smooth muscle tissue has been questioned [73].

ZIPK (DAPK3) is a member of the death-associated protein kinase (DAPK) family, which includes DAPK1, DAPK2, DAP-related protein kinase 1 (DRAK1) and DRAK2 [74,75]. Unlike other DAPK family members, ZIPK lacks a calmodulin-binding site and its activity is independent of Ca²⁺ [76]. Seven phosphorylation sites have been identified in ZIPK: T180, T225, T265, T299, T300, T306 and S311 [77]. Phosphorylation at T299, T306 and T311 has little effect on ZIPK activity, but phosphorylation at T180 (within the kinase activation loop),

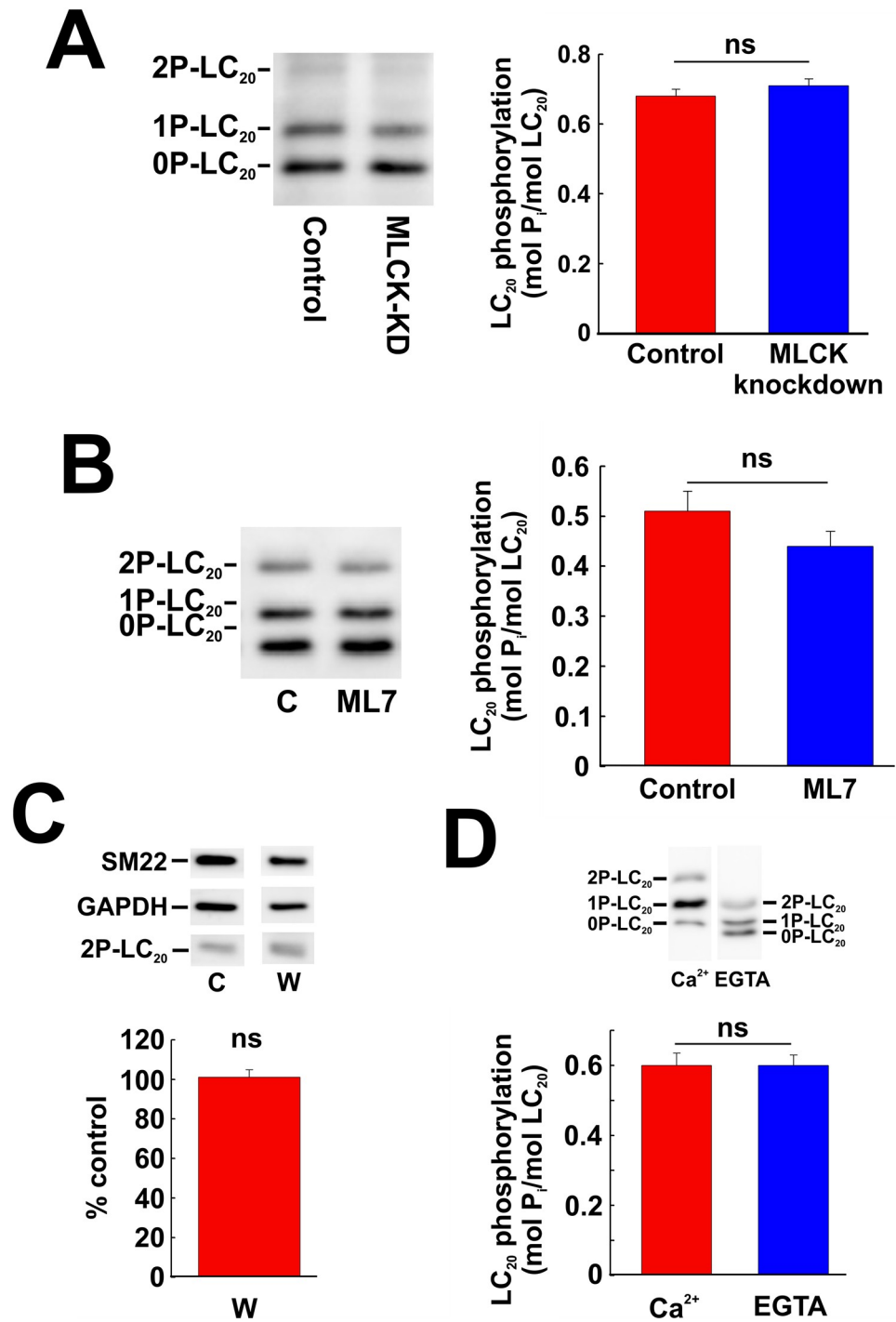


Fig 16. Effect of MLCK knockdown or inhibition on LC₂₀ phosphorylation under serum-free conditions. (A) MLCK was down-regulated in CASMC by siRNA treatment. Controls were treated identically, but with negative control siRNA. Cells were serum starved overnight prior to lysis in Laemmli sample buffer for Phos-tag SDS-PAGE and western blotting with anti-LC₂₀. A representative western blot (left-hand panel) and cumulative quantitative data (right-hand panel) are shown. Data are presented as LC₂₀ phosphorylation stoichiometry and values represent the mean ± SEM. "ns" denotes $p > 0.05$ ($n = 10$; Student's unpaired t -test). (B) Effect of ML7 (10 μ M) treatment on LC₂₀ phosphorylation (analysed by Phos-tag SDS-PAGE and western blotting with anti-LC₂₀) in the absence of serum stimulation. Controls (C) were incubated with vehicle rather than ML7. A representative western blot is shown in the left-hand panel and overall phosphorylation stoichiometry in the right-hand panel. "ns" denotes $p > 0.05$ ($n = 6$; Dunnett's *post hoc* test). (C) Effect of wortmannin (1 μ M) treatment on LC₂₀ diphosphorylation (analysed by western

blotting with anti-2P-LC₂₀: representative western blots are shown in the upper panel with cumulative quantitative data in the lower panel. “ns” denotes $p > 0.05$ ($p = 0.8633$; $n = 11$; Student’s unpaired t -test). (D) Effect of chelation of Ca²⁺ with EGTA on LC₂₀ phosphorylation under serum-free conditions. CASC were incubated in medium containing Ca²⁺ (2.5 mM) or EGTA (5 mM) under serum-free conditions prior to Phos-tag SDS-PAGE and western blotting with anti-LC₂₀. A representative western blot is shown in the upper panel with quantitative data depicted in the lower panel. “ns” denotes $p > 0.05$ (Student’s unpaired t -test).

<https://doi.org/10.1371/journal.pone.0226406.g016>

T225 (in the substrate-binding groove) and T265 (in kinase subdomain X) is essential for full kinase activation [45]. ROCK also phosphorylates ZIPK at multiple sites leading to its activation [45,77–79], and our results provide additional evidence for the integration of ZIPK and ROCK signaling networks at the cellular level.

Arterial smooth muscle cells undergo dedifferentiation when cultured, which involves transition from a non-proliferative, contractile phenotype to a proliferative, motile phenotype [80]. These changes reflect similar changes occurring in arterial smooth muscle cells *in situ* that contribute to cardiovascular diseases such as atherosclerosis [81]. The major goals of this study were to characterize the time courses of serum-induced phosphorylation events relevant to contractility, migration and cytokinesis of human cultured arterial smooth muscle cells [48], with an emphasis on LC₂₀ diphosphorylation and the kinases responsible, directly and indirectly, for its phosphorylation. We used two experimental approaches to investigate ROCK and ZIPK as likely candidates in the diphosphorylation of LC₂₀ as well as MYPT1 and Par-4 phosphorylation in response to serum treatment: (i) siRNA-mediated knockdown of ROCK and ZIPK, and (ii) inhibition of kinase activity by well-characterized and selective inhibitors (GSK429286A and H1152 for ROCK and HS38 for ZIPK).

Exposure of serum-starved cells to serum resulted in the rapid phosphorylation of LC₂₀ at T18 and S19 (Figs 1 and 2). Similar time courses of serum-induced phosphorylation of MYPT1 at T696 and T853 (Fig 3) and of Par-4 at T163 (Fig 4) were observed, both of which result in inhibition of MLCP activity [72,82], suggesting that the rapid diphosphorylation of LC₂₀ is a consequence of activation of a kinase(s) that directly phosphorylates LC₂₀ with the concomitant inhibition of MLCP activity. Furthermore, LC₂₀ phosphorylation at both T18 and S19 reduces the rate of LC₂₀ dephosphorylation by MLCP compared to that of LC₂₀ phosphorylated exclusively at S19 [10]. This helps to explain the observed sustained phosphorylation of LC₂₀.

The most obvious candidate kinase for the serum-induced phosphorylation of LC₂₀ was MLCK itself. While S19 is the site of phosphorylation responsible for smooth muscle contraction, MLCK is well known to be capable of phosphorylating T18 as well [5]. As noted in the Introduction, however, this has only been demonstrated *in vitro* with purified MLCK at supra-physiological concentrations relative to the LC₂₀ substrate [5,6] and there is plenty of evidence to support the conclusion that *in situ* and under physiological conditions MLCK does not phosphorylate T18 [7,8,83]. Nevertheless, we investigated the potential role of MLCK in serum-induced LC₂₀ phosphorylation in CASC and found that: (i) western blot analysis confirmed the expression of smooth muscle MLCK in CASC (Fig 7A), (ii) MLCK knockdown had no effect on LC₂₀ phosphorylation at T18 or S19 (Fig 7B, 7C and 7D), although we were only able to reduce MLCK levels by ~45% (Fig 5), (iii) the MLCK inhibitors ML7 and wortmannin also had no effect on LC₂₀ phosphorylation at T18 or S19 (Fig 8), and (iv) removal of extracellular Ca²⁺ and depletion of endogenous Ca²⁺ stores with EGTA had no effect on serum-induced LC₂₀ phosphorylation at T18 or S19 (Fig 9). MLCK activity is absolutely dependent on Ca²⁺ [14]. We conclude, therefore, that MLCK does not play a role in LC₂₀ phosphorylation at T18 or S19 in response to serum treatment of CASC.

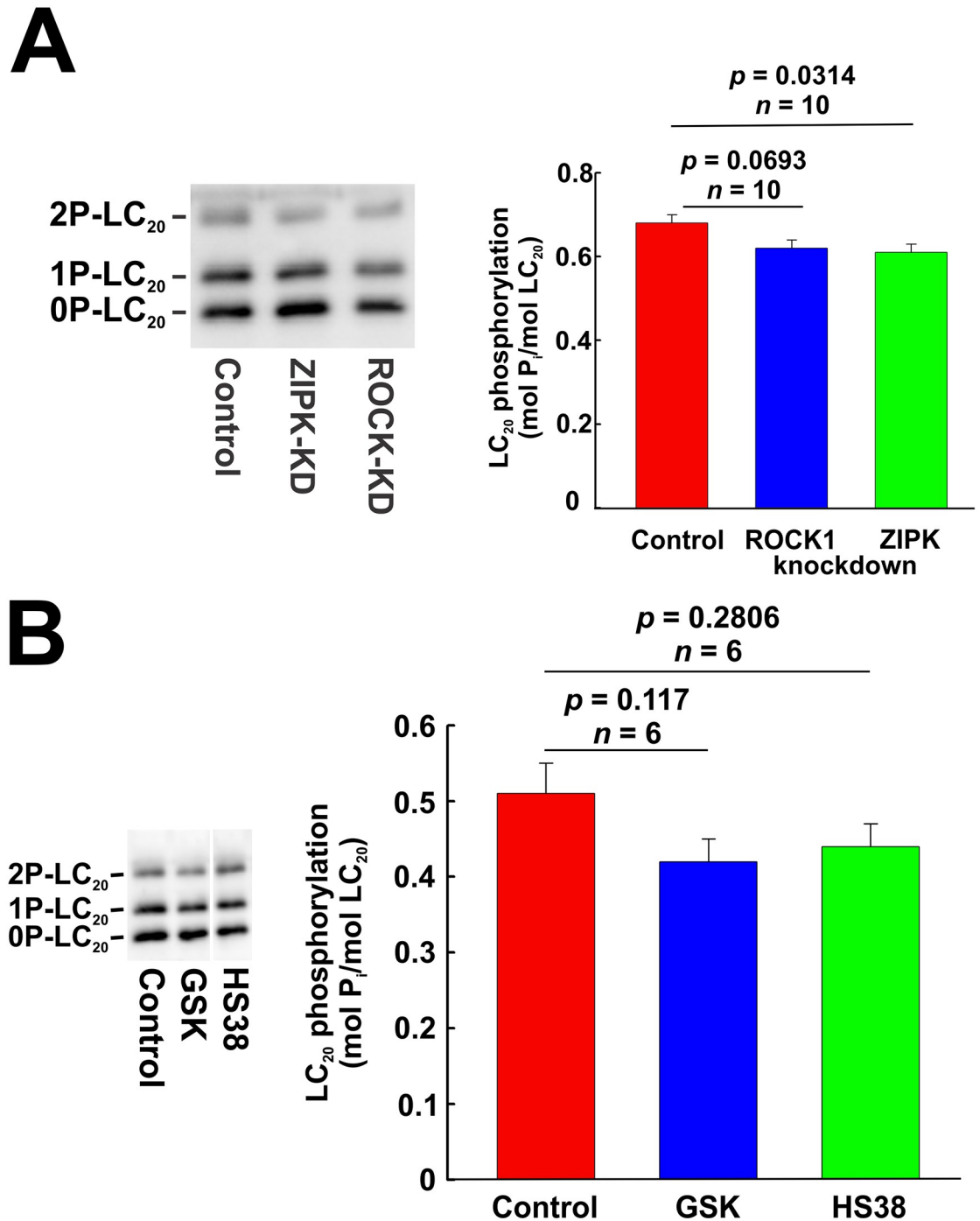


Fig 17. Effect of knockdown and inhibition of ROCK1 and ZIPK on LC₂₀ phosphorylation under serum-free conditions assessed by Phos-tag SDS-PAGE. (A) ROCK1 or ZIPK was down-regulated by siRNA treatment. Controls were treated identically, but with negative control siRNA. Cells were serum starved overnight prior to lysis in Laemmli sample buffer for Phos-tag SDS-PAGE and western blotting with anti-LC₂₀. A representative western blot is shown in the left-hand panel with cumulative quantitative data on LC₂₀ phosphorylation stoichiometry in the right-hand panel. Statistical analysis was carried out with Dunnett's *post hoc* test. (B) The effect of inhibition of ROCK or ZIPK on LC₂₀ phosphorylation in UASMC assessed by Phos-tag SDS-PAGE and western blotting with anti-LC₂₀. A representative western blot is shown in the left-hand panel with cumulative quantitative data on LC₂₀ phosphorylation stoichiometry in the right-hand panel. Statistical analysis was carried out with Dunnett's *post hoc* test.

<https://doi.org/10.1371/journal.pone.0226406.g017>

We also investigated the time courses of serum-induced phosphorylation of signaling pathway components distinct from those involved in LC₂₀ phosphorylation and its regulation, specifically Akt (S1 Fig), ERK1/2 (S2 and S3 Figs), p38 MAPK (S4A and S4B Fig) and HSP27 (S4C and S4D Fig). Phosphorylation of these proteins at activating sites was much slower than observed for LC₂₀, MYPT1 and Par-4 in both CASC and UASC.

ROCK knockdown (by 73–77%: Fig 6) reduced the serum-induced diphosphorylation of LC₂₀ at T18 and S19 and the phosphorylation of MYPT1 at T696 and T853 and of Par-4 at T163 (Fig 11). ROCK inhibition also reduced LC₂₀ diphosphorylation, Par-4 phosphorylation at T163 and MYPT1 phosphorylation at T853 but, unlike the effect of ROCK knockdown, ROCK inhibition did not affect serum-induced phosphorylation of MYPT1 at T696 (Figs 12A–12D and 13A and 13B). This suggests that ROCK knockdown down-regulates a distinct kinase that is responsible for the phosphorylation of MYPT1 at T696 whose activity is unaffected by GSK429286A. Indeed, we have shown previously that ROCK knockdown affects the expression of numerous cellular proteins [33]. ZIPK knockdown (by 45–50%) had a lesser, albeit significant effect on LC₂₀ diphosphorylation but actually increased MYPT1 and Par-4 phosphorylation (Fig 11A, 11B and 11D). The latter observation can be explained by an increase in ROCK levels due to ZIPK knockdown (Fig 6C). Depletion of ZIPK may also alleviate Par-4-mediated “lockdown” of MYPT1 inhibitory phosphorylation sites, thereby allowing for increased access to ROCK. ZIPK inhibition reduced the serum-induced increase in LC₂₀ diphosphorylation but had no effect on MYPT1 or Par-4 phosphorylation (Figs 12A, 12E and 13A and 13C).

As noted above, ZIPK activity is regulated by phosphorylation at multiple sites. Phos-tag SDS-PAGE is a very useful electrophoretic technique that separates phosphorylated forms of a protein based on the interactions of the phosphate moieties with an immobilized ligand in an SDS-polyacrylamide gel such that the higher the phosphorylation stoichiometry the slower the migration rate [35]. We have previously adapted this technique to the analysis of various phosphoproteins, e.g., MYPT1 [84], and in the current work to the phosphorylation of ZIPK. Using Phos-tag SDS-PAGE, we demonstrated that serum treatment of CASC and UASC induced a rapid increase in ZIPK phosphorylation at up to four sites (Fig 14). ROCK knockdown inhibited serum-induced ZIPK phosphorylation (Fig 15A), confirming ROCK-mediated phosphorylation of ZIPK originally identified by Haystead’s group [78], while ZIPK knockdown reduced ZIPK levels but did not have a significant effect on ZIPK phosphorylation in response to serum treatment (Fig 15A). Inhibitors of ROCK (GSK429286A) and ZIPK (HS38) individually reduced the serum-induced phosphorylation of ZIPK, with ROCK inhibition having a larger effect (Fig 15B and 15C). ROCK and ZIPK inhibitors together abolished serum-induced ZIPK phosphorylation (Fig 15D). We conclude that ROCK is the predominant kinase responsible for ZIPK phosphorylation in response to serum treatment with additional contribution from ZIPK autophosphorylation.

We used the same strategy combining kinase knockdown and pharmacological inhibitors to investigate the potential roles of MLCK, ROCK and ZIPK in LC₂₀ phosphorylation under serum-free conditions (Figs 16 and 17) and concluded that none of these kinases could account for the basal level of LC₂₀ phosphorylation that is observed in the absence of serum stimulation.

Our principal conclusion from these studies is that ROCK plays a major role in serum-induced phosphorylation of LC₂₀ at T18 and S19, phosphorylation of MYPT1 at T853 and of Par-4 at T163, whereas ZIPK plays a lesser role in serum-induced diphosphorylation of LC₂₀ and does not phosphorylate MYPT1 or Par-4 (Fig 18). Finally, our results indicate the importance of considering ZIPK and ROCK as integrated signaling molecules when interpreting the

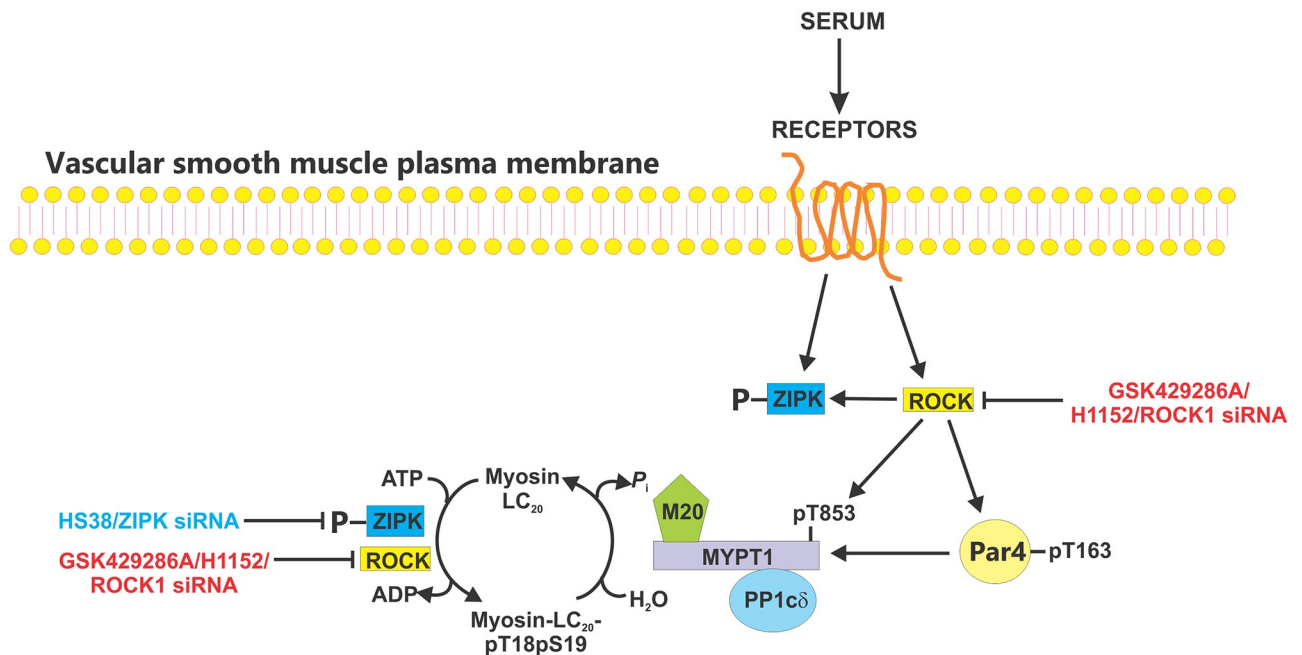


Fig 18. Summary of key findings. A schematic showing the main conclusions from this study regarding serum-induced phosphorylation of the regulatory light chains of myosin II (LC₂₀) and the regulatory kinases and phosphatase involved. Serum treatment of CASMC and UASMC activates Rho-associated coiled-coil kinase (ROCK) and zipper-interacting protein kinase (ZIPK) leading to phosphorylation of the regulatory myosin-targeting subunit (MYPT1) of myosin light chain phosphatase (MLCP) at T853 and prostate apoptosis response 4 (Par4) at T163, both of which result in inhibition of MLCP activity. ZIPK activation involves phosphorylation by ROCK and autophosphorylation. Activated ROCK and ZIPK directly phosphorylate LC₂₀ at T18 and S19.

<https://doi.org/10.1371/journal.pone.0226406.g018>

results of experiments that use genetic knockdown and/or pharmacological inhibition of the kinases.

Supporting information

S1 Fig. Time courses of serum-induced Akt phosphorylation at S473 in human arterial smooth muscle cells. Human coronary (A) and umbilical arterial smooth muscle cells (B) were treated with serum at time zero, as described in the legend to Fig 1. Cells were lysed in Laemmli sample buffer at the indicated times and subjected to SDS-PAGE and western blotting with anti-pS473-Akt. Representative western blots are shown above cumulative quantitative data in each panel. Phospho-Akt signals were normalized to GAPDH and expressed relative to the pAkt: GAPDH ratio at time zero. Values indicate the mean ± SEM (*n* = 12 (A); *n* = 9 (B)). Significant differences from the value at time zero are indicated with their respective *p* values (Dunnett's *post hoc* test). (PDF)

S2 Fig. Time courses of serum-induced ERK phosphorylation at T202/Y204 (ERK1) or T185/Y187 (ERK2) in human coronary arterial smooth muscle cells. Human coronary arterial smooth muscle cells were treated with serum at time zero, as described in the legend to Fig 1. Cells were lysed in Laemmli sample buffer at the indicated times and subjected to SDS-PAGE and western blotting with anti-pT202/pY204 (ERK1)/anti-pT185/pY187 (ERK2). Representative western blots are shown (A) with cumulative quantitative data for pERK1 (B) and pERK2 (C). Phospho-ERK signals were normalized to GAPDH and expressed relative to the pERK: GAPDH ratio at time zero. Values indicate the mean ± SEM (*n* = 8). Significant

differences from the value at time zero are indicated with the actual p value or $*p < 0.0001$ (Dunnett's *post hoc* test).

(PDF)

S3 Fig. Time course of serum-induced ERK1/2 phosphorylation at T202/Y204 and T185/Y187 in human umbilical arterial smooth muscle cells. Human umbilical arterial smooth muscle cells were treated with serum at time zero, as described in the legend to Fig 1. Cells were lysed in Laemmli sample buffer at the indicated times and subjected to SDS-PAGE and western blotting with anti-pT202/pY204 (ERK1)/anti-pT185/pY187 (ERK2). Representative western blots are shown above cumulative quantitative data. Phospho-ERK signals were normalized to GAPDH and expressed relative to the pERK: GAPDH ratio at time zero. Values indicate the mean \pm SEM ($n = 9$). Significant differences from the value at time zero are indicated with their respective p values (Dunnett's *post hoc* test).

(PDF)

S4 Fig. Time courses of serum-induced p38 MAP kinase phosphorylation at T180 and Y182 and HSP27 phosphorylation at S82 in human arterial smooth muscle cells. Human coronary (A, C) and umbilical arterial smooth muscle cells (B, D) were treated with serum at time zero, as described in the legend to Fig 1. Cells were lysed in Laemmli sample buffer at the indicated times and subjected to SDS-PAGE and western blotting with anti-pT180/pY182-p38 MAP kinase (A, B) or anti-pS82-HSP27 (C, D). Representative western blots are shown above cumulative quantitative data in each panel. Phospho-p38 MAP kinase signals were normalized to SM22 and expressed relative to the phospho-p38 MAP kinase: SM22 ratio at time zero (A, B). Phospho-HSP27 signals were normalized to GAPDH and expressed relative to the pHSP27: GAPDH ratio at time zero. Values indicate the mean \pm SEM ($n = 7$). Statistically significant differences from the value at time zero are indicated with their respective p values (Dunnett's *post hoc* test). No statistically significant differences were detected in panel D.

(PDF)

S5 Fig. Verification of wortmannin inhibition of Akt phosphorylation. CASMC were serum starved overnight in the presence of H1152 (1 μ M), GSK429286A (GSK; 1 μ M), wortmannin (1 μ M) or vehicle (control). Cells were lysed in Laemmli sample buffer for SDS-PAGE and western blotting with anti-pS473-Akt. Representative western blots are shown in panel A with cumulative quantitative data in panel B. Statistical analysis was carried out with Dunnett's *post hoc* test.

(PDF)

Author Contributions

Conceptualization: Jing-Ti Deng, Justin A. MacDonald, Michael P. Walsh.

Data curation: Cindy Sutherland.

Formal analysis: Cindy Sutherland, Justin A. MacDonald, Michael P. Walsh.

Funding acquisition: Justin A. MacDonald, Michael P. Walsh.

Investigation: Jing-Ti Deng, Sabreena Bhaidani, Cindy Sutherland.

Methodology: Jing-Ti Deng, Sabreena Bhaidani, Cindy Sutherland, Michael P. Walsh.

Project administration: Justin A. MacDonald, Michael P. Walsh.

Resources: Justin A. MacDonald, Michael P. Walsh.

Supervision: Justin A. MacDonald, Michael P. Walsh.

Validation: Sabreena Bhaidani, Cindy Sutherland, Michael P. Walsh.

Visualization: Jing-Ti Deng, Cindy Sutherland, Michael P. Walsh.

Writing – original draft: Michael P. Walsh.

Writing – review & editing: Jing-Ti Deng, Sabreena Bhaidani, Cindy Sutherland, Justin A. MacDonald, Michael P. Walsh.

References

1. Hartshorne DJ. Biochemistry of the contractile process in smooth muscle. In: Johnson LR, editor. Physiology of the gastrointestinal tract. New York: Raven Press; 1987. pp. 423–482.
2. Allen BG, Walsh MP (1994) The biochemical basis of the regulation of smooth-muscle contraction. *Trends Biochem Sci* 19: 362–368. [https://doi.org/10.1016/0968-0004\(94\)90112-0](https://doi.org/10.1016/0968-0004(94)90112-0) PMID: 7985229
3. Gallagher PJ, Herring PB, Stull JT (1997) Myosin light chain kinases. *J Muscle Res Cell Motil* 18: 1–16. <https://doi.org/10.1023/a:1018616814417> PMID: 9147985
4. Kamm KE, Stull JT (2001) Dedicated myosin light chain kinases with diverse cellular functions. *J Biol Chem* 276: 4527–4530. <https://doi.org/10.1074/jbc.R000028200> PMID: 11096123
5. Ikebe M, Hartshorne DJ (1985) Phosphorylation of smooth muscle myosin at two distinct sites by myosin light chain kinase. *J Biol Chem* 260: 10027–10031. PMID: 3839510
6. Ikebe M, Hartshorne DJ, Elzinga M (1986) Identification, phosphorylation, and dephosphorylation of a second site for myosin light chain kinase on the 20,000-Dalton light chain of smooth muscle myosin. *J Biol Chem* 261: 36–39. PMID: 3079756
7. Mita M, Yanagihara H, Hishinuma S, Saito M, Walsh MP (2002) Membrane depolarization-induced contraction of rat caudal arterial smooth muscle involves Rho-associated kinase. *Biochem J* 364: 431–440. <https://doi.org/10.1042/BJ20020191> PMID: 12023886
8. Wilson DP, Sutherland C, Walsh MP (2002) Ca²⁺ activation of smooth muscle contraction. Evidence for the involvement of calmodulin that is bound to the Triton-insoluble fraction even in the absence of Ca²⁺. *J Biol Chem* 277: 2186–2192. <https://doi.org/10.1074/jbc.M110056200> PMID: 11707462
9. Takeya K, Wang X, Kathol I, Loutzenhiser K, Loutzenhiser R, et al. (2014) Endothelin-1, but not angiotensin II, induces afferent arteriolar myosin diphosphorylation as a potential contributor to prolonged vasoconstriction. *Kidney Int* 87: 370–381. <https://doi.org/10.1038/ki.2014.284> PMID: 25140913
10. Sutherland C, Walsh MP (2012) Myosin regulatory light chain diphosphorylation slows relaxation of arterial smooth muscle. *J Biol Chem* 287: 24064–24076. <https://doi.org/10.1074/jbc.M112.371609> PMID: 22661704
11. Sasaki Y, Iwata K, Sasaki Y (1990) Concanavalin A- and fetal-calf-serum-induced rounding and myosin light chain phosphorylation in cultured smooth muscle cells. *J Cell Physiol* 144: 183–189. <https://doi.org/10.1002/jcp.1041440202> PMID: 2116423
12. Sakurada K, Seto M, Sasaki Y (1998) Dynamics of myosin light chain phosphorylation at Ser19 and Thr18/Ser19 in smooth muscle cells in culture. *Am J Physiol Cell Physiol* 274: C1563–C1572.
13. Hirano M, Hirano K (2016) Myosin di-phosphorylation and peripheral actin bundle formation as initial events during endothelial barrier disruption. *Sci Reports* 6: 20989.
14. Weber LP, Van Lierop JE, Walsh MP (1999) Ca²⁺-independent phosphorylation of myosin in rat caudal artery and chicken gizzard myofilaments. *J Physiol* 516: 805–824. <https://doi.org/10.1111/j.1469-7793.1999.0805u.x> PMID: 10200427
15. Amano M, Ito M, Kimura K, Fukata Y, Chihara K, et al. (1996) Phosphorylation and activation of myosin by Rho-associated kinase (Rho-kinase). *J Biol Chem* 271: 20246–20249. <https://doi.org/10.1074/jbc.271.34.20246> PMID: 8702756
16. Murata-Hori M, Suizu F, Iwasaki T, Kikuchi A, Hosoya H (1999) ZIP kinase identified as a novel myosin regulatory light chain kinase in HeLa cells. *FEBS Lett* 451: 81–84. [https://doi.org/10.1016/s0014-5793\(99\)00550-5](https://doi.org/10.1016/s0014-5793(99)00550-5) PMID: 10356987
17. Murata-Hori M, Fukuta Y, Ueda K, Iwasaki T, Hosoya H (2001) HeLa ZIP kinase induces diphosphorylation of myosin II regulatory light chain and reorganization of actin filaments in nonmuscle cells. *Oncogene* 20: 8175–8183. <https://doi.org/10.1038/sj.onc.1205055> PMID: 11781833

18. Niiro N, Ikebe M (2001) Zipper-interacting protein kinase induces Ca^{2+} free smooth muscle contraction via myosin light chain phosphorylation. *J Biol Chem* 276: 29567–29574. <https://doi.org/10.1074/jbc.M102753200> PMID: 11384979
19. Komatsu S, Ikebe M (2004) ZIP kinase is responsible for the phosphorylation of myosin II and necessary for cell motility in mammalian fibroblasts. *J Cell Biol* 165: 243–254. <https://doi.org/10.1083/jcb.200309056> PMID: 15096528
20. Moffat L, Brown S, Grassie M, Ulke-Lemée A, Williamson L, et al. (2011) Chemical genetics of zipper-interacting protein kinase reveal myosin light chain as a *bone fide* substrate in permeabilized arterial smooth muscle. *J Biol Chem* 286: 36978–36991. <https://doi.org/10.1074/jbc.M111.257949> PMID: 21880706
21. Deng JT, Van Lierop JE, Sutherland C, Walsh MP (2001) Ca^{2+} -independent smooth muscle contraction. A novel function for integrin-linked kinase. *J Biol Chem* 276: 16365–16373. <https://doi.org/10.1074/jbc.M011634200> PMID: 11278951
22. Wilson DP, Sutherland C, Borman MA, Deng JT, MacDonald JA, et al. (2005a) Integrin-linked kinase is responsible for Ca^{2+} -independent myosin diphosphorylation and contraction of vascular smooth muscle. *Biochem J* 392: 641–648. <https://doi.org/10.1042/BJ20051173> PMID: 16201970
23. Yamashiro S, Totsukawa G, Yamakita Y, Sasaki Y, Madaule P, et al. (2003) Ctrk kinase, a Rho-dependent kinase, induces di-phosphorylation of regulatory light chain of myosin II. *Mol Biol Cell* 14: 1745–1756. <https://doi.org/10.1091/mbc.E02-07-0427> PMID: 12802051
24. Tamura M, Nakao H, Yoshizaki H, Shiratsuchi M, Shigyo H, et al. (2005) Development of specific Rho-kinase inhibitors and their clinical application. *Biochim Biophys Acta* 1754: 245–252. <https://doi.org/10.1016/j.bbapap.2005.06.015> PMID: 16213195
25. Bain J, Plater L, Elliott M, Shpiro N, Hastie CJ, et al. (2007) The selectivity of protein kinase inhibitors: a further update. *Biochem J* 408: 297–315. <https://doi.org/10.1042/BJ20070797> PMID: 17850214
26. Nichols RJ, Dzamko N, Hutti JE, Cantley LC, Deak M, et al. (2009) Substrate specificity and inhibitors of LRRK2, a protein kinase mutated in Parkinson's disease. *Biochem J* 424: 47–60. <https://doi.org/10.1042/BJ20091035> PMID: 19740074
27. Carlson DA, Franke AS, Weitzel DH, Speer BL, Hughes PF, et al. (2013) Fluorescence linked enzyme chemoproteomic strategy for discovery of a potent and selective DAPK1 and ZIPK inhibitor. *ACS Chem Biol* 8: 2715–2723. <https://doi.org/10.1021/cb400407c> PMID: 24070067
28. MacDonald JA, Sutherland C, Carlson DA, Bhaidani S, Al-Ghabkari A, et al. (2016) A small molecule pyrazolo[3,4-d]pyrimidinone inhibitor of zipper-interacting protein kinase suppresses calcium sensitization of vascular smooth muscle. *Mol Pharmacol* 89: 105–117. <https://doi.org/10.1124/mol.115.100529> PMID: 26464323
29. Al-Ghabkari A, Deng JT, McDonald PC, Dedhar S, Alshehri M, et al. (2016) A novel inhibitory effect of oxazol-5-one compounds on ROCKII signaling in human coronary artery vascular smooth muscle cells. *Sci Rep* 6: 32118. <https://doi.org/10.1038/srep32118> PMID: 27573465
30. Okamoto M, Takayama K, Shimizu T, Ishida K, Takahashi O, et al. (2009) Identification of death-associated protein kinase inhibitors using structure-based virtual screening. *J Med Chem* 52: 7323–7327. <https://doi.org/10.1021/jm901191q> PMID: 19877644
31. Davies SP, Reddy H, Caivano M, Cohen P (2000) Specificity and mechanism of action of some commonly used protein kinase inhibitors. *Biochem J* 351: 95–105. <https://doi.org/10.1042/0264-6021:3510095> PMID: 10998351
32. Bain J, McLauchlan H, Elliott M, Cohen P (2003) The specificities of protein kinase inhibitors: an update. *Biochem J* 371: 199–204. <https://doi.org/10.1042/BJ20021535> PMID: 12534346
33. Deng JT, Wang XL, Chen YX, O'Brien ER, Gui Y, et al. (2015) The effects of knockdown of Rho-associated kinase 1 and zipper-interacting protein kinase in gene expression and function in cultured human arterial smooth muscle cells. *PLoS ONE* 10(2): e0116969. <https://doi.org/10.1371/journal.pone.0116969> PMID: 25723491
34. Paul ER, Ngai PK, Walsh MP, Gröschel-Stewart U (1995) Embryonic chicken gizzard: expression of the smooth muscle regulatory proteins caldesmon and myosin light chain kinase. *Cell Tissue Res* 279: 331–337. <https://doi.org/10.1007/bf00318489> PMID: 7895272
35. Kinoshita E, Kinoshita-Kikuta E, Takiyama K, Koike T (2006) Phosphate-binding tag, a new tool to visualize phosphorylated proteins. *Mol Cell Proteomics* 5: 749–757. <https://doi.org/10.1074/mcp.T500024-MCP200> PMID: 16340016
36. Shiojima I, Walsh K (2002) Role of Akt signaling in vascular homeostasis and angiogenesis. *Circ Res* 90: 1243–1250. <https://doi.org/10.1161/01.res.0000022200.71892.9f> PMID: 12089061
37. Morello F, Perino A, Hirsch E (2009) Phosphoinositide 3-kinase signalling in the vascular system. *Cardiovasc Res* 82: 261–271. <https://doi.org/10.1093/cvr/cvn325> PMID: 19038971

38. Risso G, Blaustein M, Pozzi B, Mammi P, Srebrow A (2015) Akt/PKB: one kinase, many modifications. *Biochem J* 468: 203–214. <https://doi.org/10.1042/BJ20150041> PMID: 25997832
39. Johnson GL, Lapadat R (2002) Mitogen-activated protein kinase pathways mediated by ERK, JNK, and p38 protein kinases. *Science* 298: 1911–1912. <https://doi.org/10.1126/science.1072682> PMID: 12471242
40. Huang C, Jacobson K, Schaller MD (2004) MAP kinases and cell migration. *J Cell Sci* 117: 4619–4628. <https://doi.org/10.1242/jcs.01481> PMID: 15371522
41. Herlaar E, Brown Z (1999) p38 MAPK signaling cascades in inflammatory disease. *Mol Med Today* 5: 439–447. [https://doi.org/10.1016/s1357-4310\(99\)01544-0](https://doi.org/10.1016/s1357-4310(99)01544-0) PMID: 10498912
42. Kostenko S, Moens U (2009) Heat shock protein 27 phosphorylation: kinases, phosphatases, functions and pathology. *Cell Mol Life Sci* 66: 3289–3307. <https://doi.org/10.1007/s00018-009-0086-3> PMID: 19593530
43. Salinthon S, Tyagi M, Gerthoffer WT (2008) Small heat shock proteins in smooth muscle. *Pharmacol Ther* 119: 44–54. <https://doi.org/10.1016/j.pharmthera.2008.04.005> PMID: 18579210
44. Wilson DP, Susnjar M, Kiss E, Sutherland C, Walsh MP (2005b) Thromboxane A₂-induced contraction of rat caudal arterial smooth muscle involves activation of Ca²⁺ entry and Ca²⁺ sensitization: Rho-associated kinase-mediated phosphorylation of MYPT1 at Thr-855 but not Thr-697. *Biochem J* 389: 763–774. <https://doi.org/10.1042/BJ20050237> PMID: 15823093
45. Graves PR, Winkfield KM, Haystead TAJ (2005) Regulation of zipper-interacting protein kinase activity *in vitro* and *in vivo* by multisite phosphorylation. *J Biol Chem* 280: 9363–9374. <https://doi.org/10.1074/jbc.M412538200> PMID: 15611134
46. Somlyo AP, Somlyo AV (2000) Signal transduction by G-proteins, Rho-kinase and protein phosphatase to smooth muscle and non-muscle myosin II. *J Physiol* 522: 177–185. <https://doi.org/10.1111/j.1469-7793.2000.t01-2-00177.x> PMID: 10639096
47. MacDonald JA, Walsh MP, Cole WC. Calcium sensitization in smooth muscle involving regulation of myosin light chain phosphatase activity. In: Trebak M and Earley S, editors. *Signal transduction and smooth muscle*. Boca Raton, Florida: CRC Press; 2018. pp. 123–154.
48. Fukata Y, Amano M, Kaibuchi K (2001) Rho-Rho-kinase pathway in smooth muscle contraction and cytoskeletal reorganization of non-muscle cells. *Trends Pharmacol Sci* 22: 32–39. [https://doi.org/10.1016/s0165-6147\(00\)01596-0](https://doi.org/10.1016/s0165-6147(00)01596-0) PMID: 11165670
49. Riento K, Ridley AJ (2003) ROCKs: Multifunctional kinases in cell behaviour. *Nat Rev Cell Biol* 4: 446–456.
50. Haystead TA (2005) ZIP kinase, a key regulator of myosin protein phosphatase 1. *Cell Signal* 17: 1313–1322. <https://doi.org/10.1016/j.cellsig.2005.05.008> PMID: 16005610
51. Ihara E, MacDonald JA (2007) The regulation of smooth muscle contractility by zipper-interacting protein kinase. *Can J Physiol Pharmacol* 85: 79–87. <https://doi.org/10.1139/y06-103> PMID: 17487247
52. Usui T, Okada M, Yamawaki H (2013) Zipper-interacting protein kinase (ZIPK): function and signaling. *Apoptosis* 19: 387–391.
53. Kureishi Y, Kobayashi S, Amano M, Kimura K, Kanaide H, et al. (1997) Rho-associated kinase directly induces smooth muscle contraction through myosin light chain phosphorylation. *J Biol Chem* 272: 12257–12260. <https://doi.org/10.1074/jbc.272.19.12257> PMID: 9139666
54. Borman MA, MacDonald JA, Murányi A, Hartshorne DJ, Haystead TAJ. (2002) Smooth muscle myosin phosphatase-associated kinase induces Ca²⁺ sensitization via myosin phosphatase inhibition. *J Biol Chem* 277: 23441–23446. <https://doi.org/10.1074/jbc.M201597200> PMID: 11976330
55. Al-Ghabkari A, Moffat LD, Walsh MP, MacDonald JA (2018) Validation of chemical genetics for the study of zipper-interacting protein kinase signaling. *Proteins* 86: 1211–1217. <https://doi.org/10.1002/prot.25607> PMID: 30381843
56. Kitazawa T, Kobayashi S, Horiuti K, Somlyo AV, Somlyo AP (1989) Receptor-coupled, permeabilized smooth muscle. Role of the phosphatidylinositol cascade, G-proteins, and modulation of the contractile response to Ca²⁺. *J Biol Chem* 264: 5339–5342. PMID: 2494163
57. Kitazawa T, Somlyo AP (1991) Modulation of Ca²⁺ sensitivity by agonists in smooth muscle. *Adv Exp Biol Med* 304: 97–109.
58. Kitazawa T, Masuo M, Somlyo AP (1991) G protein-mediated inhibition of myosin light-chain phosphatase in vascular smooth muscle. *Proc Natl Acad Sci USA* 88: 9307–9310. <https://doi.org/10.1073/pnas.88.20.9307> PMID: 1656467
59. Kubota Y, Nomura M, Kamm KE, Mumby MC, Stull JT (1992) GTP gamma S-dependent regulation of smooth muscle contractile elements. *Am J Physiol Cell Physiol* 262: C405–C410.

60. Masuo M, Reardon S, Ikebe M, Kitazawa T (1994) A novel mechanism for the Ca^{2+} -sensitizing effect of protein kinase C on vascular smooth muscle: Inhibition of myosin light chain phosphatase. *J Gen Physiol* 104: 265–286. <https://doi.org/10.1085/jgp.104.2.265> PMID: 7807049
61. Iizuka Y, Yoshii A, Samizo K, Tsukagoshi H, Ishizuka T, et al. (1999) A major role for the Rho-associated coiled coil forming protein kinase in G-protein-mediated Ca^{2+} sensitization through inhibition of myosin phosphatase in rabbit trachea. *Br J Pharmacol* 128: 925–933. <https://doi.org/10.1038/sj.bjp.0702864> PMID: 10556927
62. Swärd K, Dreja K, Susnjar M, Hellstrand P, Hartshorne DJ, et al. (2000) Inhibition of Rho-associated kinase blocks agonist-induced Ca^{2+} sensitization of myosin phosphorylation and force in guinea pig ileum. *J Physiol* 522: 33–49. <https://doi.org/10.1111/j.1469-7793.2000.0033m.x> PMID: 10618150
63. Totsukawa G, Yamakita Y, Yamashiro S, Hartshorne DJ, Sasaki Y, et al. (2000) Distinct roles of ROCK (Rho-kinase) and MLCK in spatial regulation of MLC phosphorylation for assembly of stress fibers and focal adhesions in 3T3 fibroblasts. *J Cell Biol* 150: 797–806. <https://doi.org/10.1083/jcb.150.4.797> PMID: 10953004
64. Kassianidou E, Hughes JH, Kumar S (2017) Activation of ROCK and MLCK tunes regional stress fiber formation and mechanics via preferential myosin light chain phosphorylation. *Mol Biol Cell* 28: 3832–3843. <https://doi.org/10.1091/mbc.E17-06-0401> PMID: 29046396
65. Kawano Y, Fukata Y, Oshiro N, Amano M, Nakamura T, et al. (1999) Phosphorylation of myosin-binding subunit (MBS) of myosin phosphatase by Rho-kinase in vivo. *J Cell Biol* 147: 1023–1038. <https://doi.org/10.1083/jcb.147.5.1023> PMID: 10579722
66. Feng J, Ito M, Ichikawa K, Isaka N, Nishikawa N, et al. (1999) Inhibitory phosphorylation site for Rho-associated kinase on smooth muscle myosin phosphatase. *J Biol Chem* 274: 37385–37390. <https://doi.org/10.1074/jbc.274.52.37385> PMID: 10601309
67. Katoh K, Kano Y, Amano M, Onishi H, Kaibuchi K, et al. (2001) Rho kinase-mediated contraction of isolated stress fibers. *J Cell Biol* 153: 569–584. <https://doi.org/10.1083/jcb.153.3.569> PMID: 11331307
68. Velasco G, Armstrong C, Morrice N, Frame S, Cohen P (2002) Phosphorylation of the regulatory subunit of smooth muscle protein phosphatase 1M at Thr850 induces its dissociation from myosin. *FEBS Lett* 527: 101–104. [https://doi.org/10.1016/s0014-5793\(02\)03175-7](https://doi.org/10.1016/s0014-5793(02)03175-7) PMID: 12220642
69. Ito M, Nakano T, Erdödi F, Hartshorne DJ (2004) Myosin phosphatase: structure, regulation and function. *Mol Cell Biochem* 259: 197–209. <https://doi.org/10.1023/b:mcbi.0000021373.14288.00> PMID: 15124925
70. Walsh MP, MacDonald JA (2018) Regulation of smooth muscle myosin light chain phosphatase by multisite phosphorylation of the myosin targeting subunit, MYPT1. *Cardiovasc Hematol Disord Drug Targets* 18: 4–13. <https://doi.org/10.2174/1871529X18666180326120638> PMID: 29577868
71. Ren X-D, Wang R, Li Q, Kahek LAF, Kaibuchi K, et al. (2004) Disruption of Rho signal transduction upon cell detachment. *J Cell Sci* 117: 3511–3518. <https://doi.org/10.1242/jcs.01205> PMID: 15226371
72. Vetterkind S, Lee E, Sundberg E, Poythress RH, Tao TC, et al. (2010) Par-4: a new activator of myosin phosphatase. *Mol Biol Cell* 21: 1214–1224. <https://doi.org/10.1091/mbc.E09-08-0711> PMID: 20130087
73. MacDonald JA, Moffat LD, Al-Ghabkari A, Sutherland C, Walsh MP (2013) Prostate-apoptosis response-4 phosphorylation in vascular smooth muscle. *Arch Biochem Biophys* 535: 84–90. <https://doi.org/10.1016/j.abb.2012.11.009> PMID: 23219599
74. Kawai T, Matsunoto M, Takeda K, Sanjo H, Akira S (1998) ZIPK, a novel serine/threonine kinase which mediates apoptosis. *Mol Cell Biol* 18: 1642–1651. <https://doi.org/10.1128/mcb.18.3.1642> PMID: 9488481
75. Shani G, Marash L, Gozuacik D, Bialik S, Teitelbaum L, et al. (2004) Death-associated protein kinase phosphorylates ZIP kinase, forming a unique kinase hierarchy to activate its cell death functions. *Mol Cell Biol* 24: 8611–8626. <https://doi.org/10.1128/MCB.24.19.8611-8626.2004> PMID: 15367680
76. Usui T, Sakatsume T, Nijima R, Otani K, Kazama K, et al. (2014) Death-associated protein kinase 3 mediates vascular structural remodelling via stimulating smooth muscle cell proliferation and migration. *Clin Sci* 127: 539–548. <https://doi.org/10.1042/CS20130591> PMID: 24814693
77. Sato N, Kamada N, Muromoto R, Kawai T, Sugiyama K, et al. (2006) Phosphorylation of threonine-265 in zipper-interacting protein kinase plays an important role in its activity and is induced by IL-6 family cytokines. *Immunol Lett* 103: 127–134. <https://doi.org/10.1016/j.imlet.2005.10.015> PMID: 16325270
78. Hagerty L, Weitzel DH, Chambers J, Fortner CN, Brush MH, et al. (2007) ROCK1 phosphorylates and activates zipper-interacting protein kinase. *J Biol Chem* 282: 4884–4893. <https://doi.org/10.1074/jbc.M609990200> PMID: 17158456

79. Hamao K, Ono T, Matsushita M, Hosoya H (2019) ZIP kinase phosphorylated and activated by Rho kinase/ROCK contributes to cytokinesis in mammalian cultures cells. *Exp Cell Res* <https://doi.org/10.1016/j.yexcr.2019.111707> PMID: 31693874
80. Chamley-Campbell J, Campbell GR, Ross R (1979) The smooth muscle cell in culture. *Physiol Rev* 59: 1–61. <https://doi.org/10.1152/physrev.1979.59.1.1> PMID: 108688
81. Gomez D, Owens GK (2016) Smooth muscle cell phenotypic switching in atherosclerosis. *Cardiovasc Res* 95: 156–164.
82. Grassie ME, Sutherland C, Ulke-Lemée A, Chappellaz M, Kiss E, et al. (2012) Cross-talk between Rho-associated kinase and cyclic nucleotide-dependent kinase signaling pathways in the regulation of smooth muscle myosin light chain phosphatase. *J Biol Chem* 287: 36356–36369. <https://doi.org/10.1074/jbc.M112.398479> PMID: 22948155
83. Walsh M. P. (2011) Vascular smooth muscle myosin light chain diphosphorylation: mechanism, function and pathological implications. *IUBMB Life* 63: 987–1000. <https://doi.org/10.1002/iub.527> PMID: 21990256
84. Sutherland C, MacDonald JA, Walsh MP (2016) Analysis of phosphorylation of the myosin-targeting subunit of myosin light chain phosphatase by Phos-tag SDS-PAGE. *Am J Physiol Cell Physiol* 310: C681–C691. <https://doi.org/10.1152/ajpcell.00327.2015> PMID: 26864694